Deformation facies analysis and tectonic evolution of low-grade schists in the Joetsu region, central Japan

Ko TAKENOUCHI*

Abstract

The present study was performed to examine the detailed exhumation process of deep-sheeted materials in accretionary complexes by analysis of deformed minorstructures recorded in a low-grade schist zone, reconstructed by tracing sporadically distributed low-grade schist bodies with similar constituent rocks, metamorphism, and deformation history in the Joetsu Belt and the Western Zone of the Ashio Belt belonging to the Paleozoic to Mesozoic systems of the Inner Zone of Southwest Japan. Geometric and kinematic analyses of deformed minor- and microstructures divided the whole deformation process into two deformation phases, i.e., the earlier deformation phase (phase 1 deformation) showing a sinistral shear regime with the deformation mechanism of crystal plasticity and diffusive mass transfer, and the later deformation phase (phase 2 deformation) showing a dextral shear regime with the deformation mechanism of fracture, slip, and cataclasis. Deformation facies analysis showed the temporal and spatial sequences (deformation zoning) of the deformed minorstructures. The former showed that deformed minorstructures formed under conditions of decreasing mean ductility with time in response to rock body exhumation, and the latter showed that mean ductility represented by the assemblage of deformed minorstructures decreased with distance from the axial part of a major isoclinal syncline in the western limb. The two inverted shear regimes were caused by alternate movement of oceanic and continental plates, i.e., NE-directed oblique subduction of the oceanic plate and NE-ENE-directed oblique upthrusting being reactivation of the Hida Nappe belonging to the continental plate. The mutual movements of the two plates played an important role in the development of the accretionary complex of the Japanese Islands.

Key words: accretionary complex, Ashio Belt, deformation facies analysis, exhumation process, Joetsu Belt, low-grade schist.

---

* Fossa Magna Museum, Ichinomiya 1313, Itoigawa 941-0056, Japan
(Manuscript received 21 January, 2005; accepted 7 March, 2005)

Introduction

This paper contributed to our understanding of the following three points: 1) the exhumation process of deep-sheeted materials of an accretionary complex by two inverted shear regimes, 2) the Geology of the Joetsu region and tectonics of the Paleozoic to Mesozoic accretionary complex in the Japanese Islands, and 3) the methodology of structural analysis using deformation facies analysis. In this study, the author examined low-grade schists originating from accretionary complex materials, showing sporadic distribution in the Joetsu region on the border between Niigata and Gunma Prefectures (Fig. 1).

The exhumation process of deep-sheeted rocks in accretionary complexes is a fundamental problem when considering the development of accretionary complexes from the viewpoint of material circulation and tectonics of active plate margins. Off-scraping processes were clarified by Otsuka (1989) and Kimura and Hori (1993) in the Mino-Tamba Belt, the development of out-of-sequence thrust at shallower levels in accretionary wedges was reported by Sample and Moore (1987) and Taira et al. (1988), and underplating processes were revealed by Mackenzie et al. (1987) and Kimura and Mukai (1991) in the Shimanto Belt. However, there have been few detailed reports regarding exhumation processes of deep-sheeted rocks, elucidated by structural analysis. The exhumation process of low-grade schists reported in this paper represents an example of the exhumation of deep-sheeted rocks caused by mutual movements of oceanic and continental plates.

Due to their complex geological structures, the constituent rocks and their formation ages of the Paleozoic-Mesozoic systems in the Inner Zone of Southwest Japan, between the Kashiwazaki-Chiba Tectonic Line (Yamashita, 1995) and the Tanagura Tetonic Line, have not been clarified. This area consists of metamorphic rocks, igneous rocks, deep-sea sediments, and shallow marine and brackish water sediments, and corresponds broadly to the Hida Marginal Belt and Jurassic accretionary complex (Mino-Tamba Belt) beyond the Fossa Magna (Fig. 1). In this study, the geology of this complex area was compiled and its regional geology was proposed in correlation with the Inner Zone of Southwest Japan. Consequently, the tectonics of mutual movement of continental and oceanic plates were proposed based on the results of structural analyses of the low-grade schists.

In structural geology, Sander's element-restoration method (Sander, 1930) has been used successfully to determine the deformation histories of rocks. In 1981, Uemura proposed a novel synthetic method known as deformation facies analysis. However, the two methods are not independent from each other, with the latter based on data obtained from the former. Structural analyses of the low-grade schists were performed by fabric analysis (Sander's method) and deformation facies analysis (Uemura, 1981). The two combined structural analytical methods were very effective to clarify the tectonics of the low-grade schists in the present study.

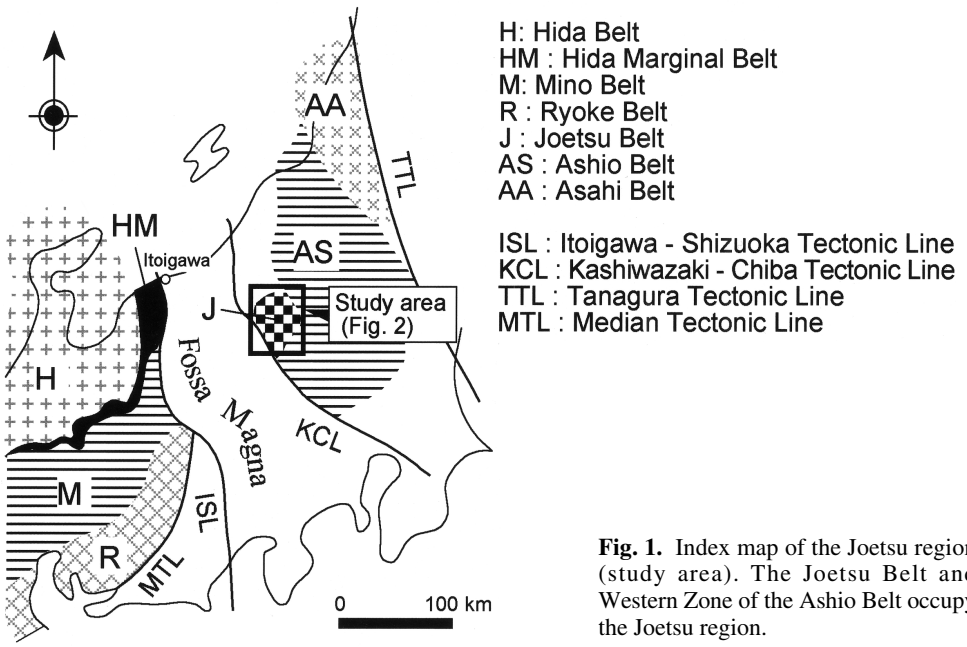

Fig. 1. Index map of the Joetsu region (study area). The Joetsu Belt and Western Zone of the Ashio Belt occupy the Joetsu region.

Outline of geology of the Joetsu region

Mesozoic to Paleozoic systems in the Inner Zone of the Southwest Japan, between the Kashiwazaki-Chiba Tectonic Line (Yamashita, 1995) and Tanagura Tectonic Line, are divided into three belts, namely, they are the Joetsu, Ashio and Asahi Belts from west to east (Fig. 1). The Joetsu Belt is characterized by metamorphic rocks, Paleozoic accretionary complex and Mesozoic to Paleozoic shallow marine and brackish water sediments in contrast to the Ashio Belt mainly consisting of Mesozoic to Paleozoic deep-sea sediments of Jurassic accretionary complex (Hayama et al., 1969; Chihara et al., 1977; Takenouchi and Takahashi, 2002). The Asahi Belt is composed of gabbroic rocks, gneissose granites, massive granites and acidic volcanics (Research Group of the Asahi Mountains, 1987; Takahashi, 1998).

Chihara and Komatsu (1982) divided the Joetsu Belt into the Tanigawadake Zone including schist-serpentinite complex and Katashina Zone including metaophiolites accompanied with Mesozoic sediments. Chihara (1984) proposed the Western Zone of the Ashio Belt, which has diagnostic mixed rocks including metabasic to ultrabasic rocks. Boundary lines between the Tanigawadake, Katashina and Ashio Western Zones are indefinite because of the lack of detailed geologic data including formative ages of the constituent rocks.

The general geological framework of the Joetsu region (border of Niigata and Gunma Prefectures) is not yet established. In this paper, geologic bodies in the Joetsu region are not classified into the conventional Tanigawadake, Katashina and Ashio Western Zones, but

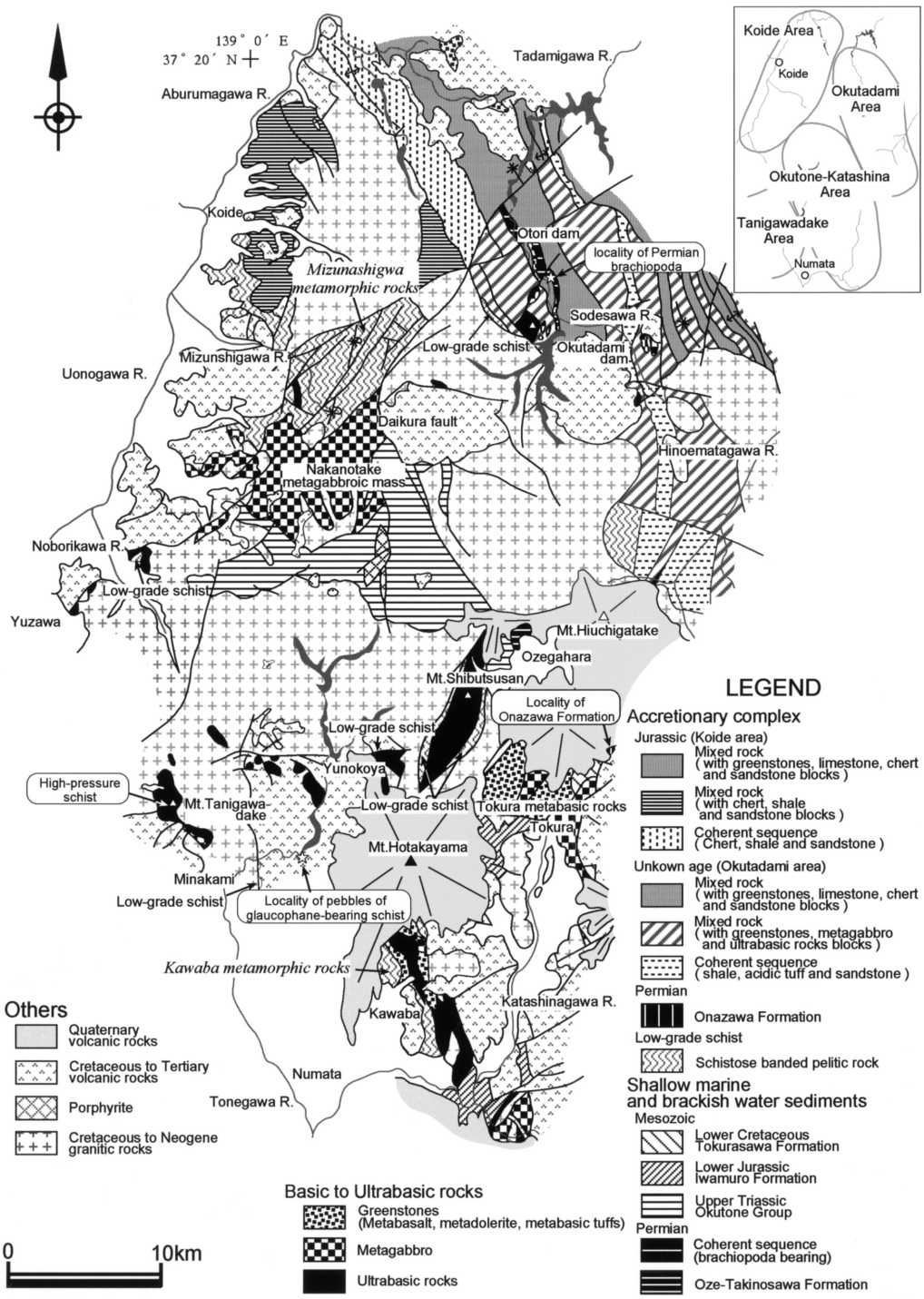

Fig. 2. Compiled geological map of the Joetsu region (modified after Takenouchi and Takahashi, 2002). Cretaceous to Neogene crustal movements including plutonism, volcanism and faulting disturbed the original zonal structure of this region. This map is compiled from Kurokawa et al. (1987), Uemura et al. (1984), Uemura and Takashima (1985), Niigata Pre-Tertiary Research Group (1986, 1996), Yamamoto et al. (2000), Takenouchi (1988), Chihara and Komatsu (1992), Chihara et al. (1981), Chihara (1985), Sato and Komatsu (1985), Sudo (1976), Yano et al. (1993), Hayama et al. (1969), Yoshimura and Ichihashi (1966) and Tazawa and Niigata Pre-Tertiary Research Group (1999).

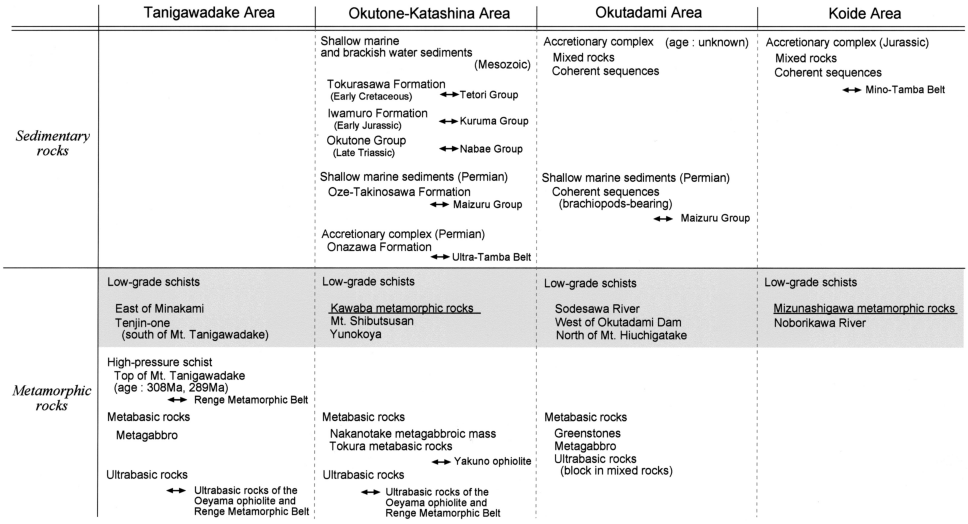

Fig. 3. Constituent rocks of the Joetsu region (after Takenouchi and Takahashi, 2002). Names of local areas are referred to Fig. 2.

describe each geologic body on the basis of their geologic characteristics. A compiled map and list of constituent rocks of the Joetsu region are shown in Figs. 2, 3.

1. Metamorphic rocks

High-pressure schists

High-pressure schist is exposed only on the top of Mt. Tanigawadake as small rock bodies within serpentinite massif (Maeda, 1962; Soma and Yoshida, 1964; Akamatsu et al., 1967). K-Ar ages of muscovite in the schist are 308±15 Ma and 284±14 Ma (Yokoyama, 1992) and suggest that the schist belong to the Hida Marginal Belt (Yokoyama, 1992) or Renge Metamorphic Belt (Shimizu et al., 2000). The evidence of schist pebbles including glaucophane (Yoshimura and Ichihashi, 1966; Shimizu et al., 2000) and phengite (Shimizu et al., 2001) in the Jurassic and Neogene formations suggests that the high-pressure schist was once exposed widely in the Joetsu region (Arai and Kizaki, 1958; Yoshimura and Ichihashi , 1966; Hayama et al., 1969; Shimizu et al., 2000, 2001). The high-pressure schist is distinguished from the low-grade schists discussed in this paper.

Metabasic rocks

Representatives of the metabasic rocks are the Nakanotake metagabbroic mass (Chihara et al., 1976) and Tokura metabasic rocks (Sato and Komatsu, 1985), which are considered to be correlative with the Yakuno ophiolite (Sato and Komatsu, 1985). The Nakanotake

metagabbroic mass consists mainly of lower cumulate rocks such as cortlandite (hornblende peridotite having hornblende host crystal including olivine and pyroxene) and pegmatite, and non-cumulate rocks such as metagabbros and amphibolite that have undergone epidote-amphibolite facies metamorphism (Chihara and Komatsu, 1992). The mass is considered to be composed of some thrust sheets bounded by schist layers (Ohkouchi et al., 2002). The Tokura metabasic rocks are composed of layered metabasic rocks, metagabbro, metabasalt to metadolerite, pillow lava to pillow breccia, chert and mixed clastic rocks (Sato and Komatsu, 1985).

Ultrabasic rocks

The Mt. Shibutsusan ultrabasic rocks are composed mainly of banded dunite and harzburgite including Cr-spinel, and are accompanied with low-grade schsits. The Tanigawadake ultrabasic rocks are composed mainly of sheared serpentinite accompanied with high-pressure schists and matagabbro (Chihara, 1985). These ultrabasic rocks may be correlated with the ultrabasic rocks of the Oeyama ophiolite and the Renge Metamorphic Belt.

Low-grade schists

Low-grade schists consist mainly of schistose banded pelitic rock having variously deformed minorstructures. The weakly developed schistosity and relatively minor recrystallization distinguish these schists from the schist of Mt. Tanigawadake.

They are the Mizunashigawa metamorphic rocks (Chihara and Nishida, 1968; Takenouchi, 1988, 2000), Kawaba metamorphic rocks (Hayama et al., 1969; Chihara, 1985) and schists of Mt. Shibutsusan associated with serpentinite (Chihara, 1985). Other small schist bodies are located to the west of the Okutadami Dam site (Chihara, 1985), to the east of Minakami (Hayama et al., 1969), on the right bank of the Noborikawa River (Chihara, 1985; Yanagisawa et al., 1986), at Yunokoya (Chihara, 1985), in the middle reaches of the Sodesawa River (Niigata Pre-Tertiary Research Group, 1986, 1996), to the north of Mt. Hiuchigatake (Yamamoto et al., 2000) and at Tenjinone to the south of Mt. Tanigawadake (Takizawa and Sato, 1986).

As discussed by Takenouchi (1988, 2000), if the Mizunashigawa metamorphic rocks belong to the Ashio Belt of Jurassic accretionary complex, part of the above schists may be correlated with the Unit III (Takami et al., 1992) of deformed lithofacies of the Kuga Group. On the other hand, Yamamoto et al. (2000) estimated the schists to be Permian accretionary complex because the schsits are adjacent to the ophiolitic rocks. Attribution of the low-grade schists will be discussed later.

2. Accretionary complexes

Permian

The Onazawa Formation, regarded as an equivalent of the Ultra-Tamba Belt (Yano et al., 1993), is composed mainly of black shale including Late Permian radiolarians associated with thin interbeds of siliceous and pelitic layers, and green sandstone (Yano et al., 1993). It is

exposed in a small area at the junction of the Katashinagawa River and Onazawa stream, northeast of Tokura.

Jurassic

Jurassic accretionary complex, considered to be correlative with the Mino-Tamba Belt (Mizutani et al., 1984), is composed of mixed rocks including various kind of blocks and coherent sequences. Cherts in the mixed rocks and coherent sequences bear Permian, Triassic and Jurassic fossils (Sato et al., 1975; Uemura et al., 1984; Uemura and Takashima, 1985; Hasegawa, 1985; Yamada and Kurokawa, 1985; Matsumoto et al., 2001; Hara and Kashiwagi, 2004).

Unknown age

A mixed rock including metabasalt, metagabbro and ultrabasic rocks is diagnostic lithofacies among the Joetsu region (Chihara, 1984; Takahashi et al., 2004). In this area (Fig. 2), no fossil age has been obtained from the shaly matrix in the mixed rocks. The Permian brachiopods-bearing coherent sequence occurs in the mixed rocks.

3. Shallow marine and brackish water sediments

Permian

The Oze-Takinosawa Formation (Yamamoto et al., 2000) is exposed north of Ozegahara marsh, and is correlated with the Maizuru Group (Yamamoto et al., 2000). This formation consists of shale and sandstone associated with minor limestone including Permian fusulinid (Fujimoto and Kobayashi, 1961).

Permian brachiopods-bearing coherent sequence consisting of interbeds of shale and acidic tuff, sandy shale and conglomerate is found from the Okutadami area (Tazawa and Niigata Pre-Tertiary Research Group, 1999). It is considered to be correlative with the Maizuru Group (Tazawa and Niigata Pre-Tertiary Research Group, 1999). However, the Permian sequence may be a large exotic block of mixed rocks whose formation age is unknown (Tazawa and Niigata Pre-Tertiary Research Group, 1999).

Mesozoic

Mesozoic shallow marine and brackish water sediments are the Upper Triassic Okutone Group (Kobayashi, 1955), Lower Jurassic Iwamuro Formation (Kimura, 1952) and Lower Cretaceous Tokurasawa Formation (Hayashi et al., 1965; Hayama et al., 1969), which are composed mainly of sandstone and shale. The Okutone Group, Iwamuro Formation and Tokurasawa Formation are considered to be correlative with the Nabae Group (Sato and Komatsu, 1985), Kuruma Group (Kimura, 1952) and Tetori Group (Hayashi et al., 1965), respectively.

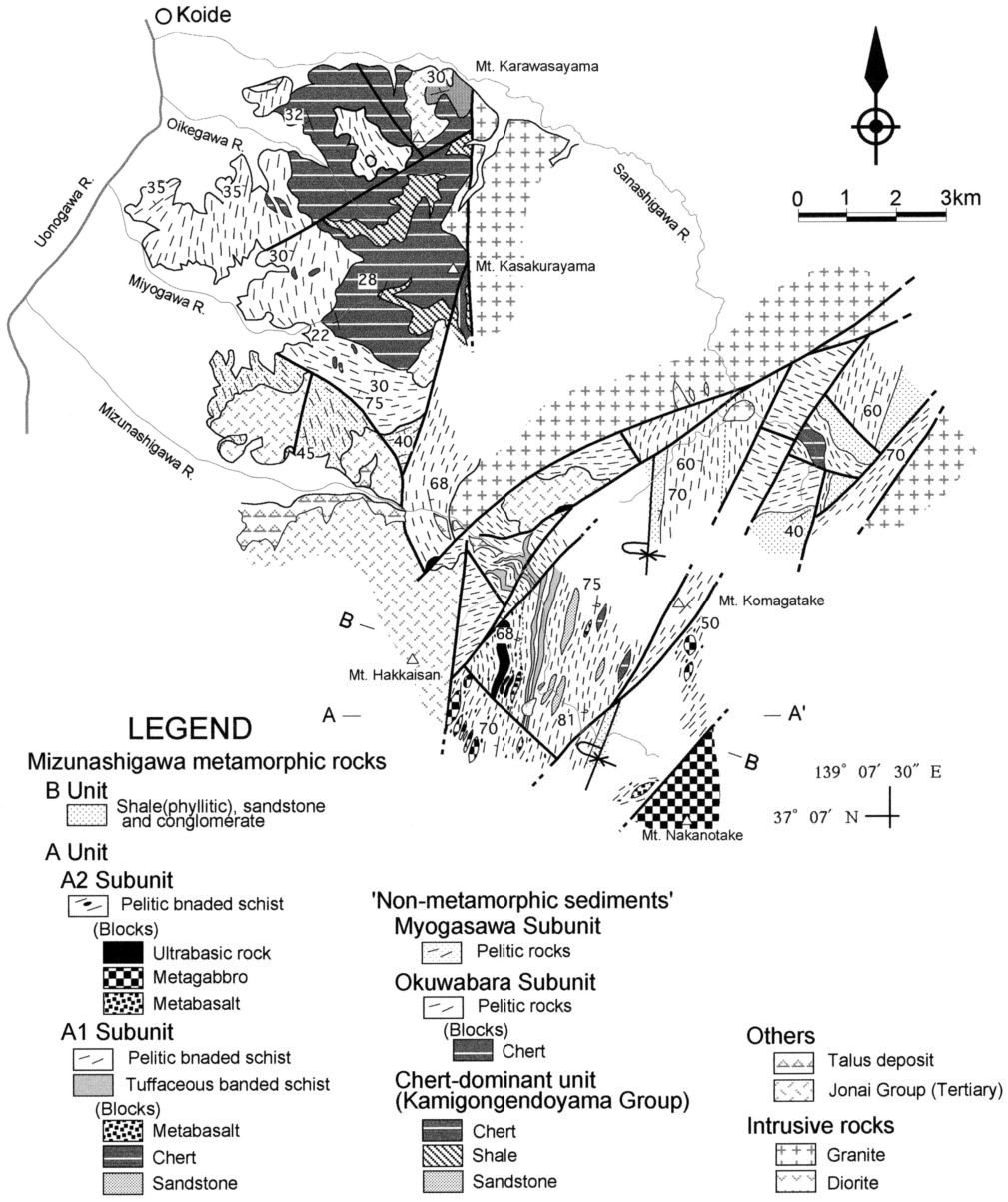

Fig. 4. Geological map of the Mizunashigawa metamorphic rocks and the non-metamorphic rocks of the Ashio Belt (modified after Takenouchi, 1988). A-A', B-B': Profile line (Fig. 5).

Geology of low-grade schists

1. Mizunashigawa metamorphic rocks

According to Takenouchi (1985, 1988), the metamorphic rocks showing mixed rock facies is composed mainly of pelitic banded schist, which has millimeter- to centimeter-scale compositional layers of white siliceous and brown pelitic layers, and includes blocks of metabasalt, metagabbro, metabasic tuff, serpentinite, chert, limestone and sandstone in size from several tens centimeters to a thousand meters. The pelitic banded schist is intercalated with tuffaceous banded schist having white siliceous layers and light-green tuffaceous layers. The compositional layers define the bedding foliation of the schists. The schists show well overprinting relationships of deformed minor and microstructures of ductile to brittle deformation.

Mineral assemblage of the schists shows muscovite-chlorite-albite-quartz, biotite-muscovite-albite-quartz and garnet-biotite-muscovite-albite-quartz in the pelitic banded schist, whereas actinolite-biotite-albite-quartz, actinolite-albite-quartz and actinolite-chlorite-albite-quartz in the tuffaceous banded schist. Above mineral assemblages indicate greenschist facies metamorphism prior to thermal metamorphism by Cretaceous to Neogene granitic intrusion.

The metamorphic rocks strike N-S to NNE-SSW and dip 60-70° W, and form an isoclinal syncline with E-vergent axial plane (Figs. 4, 5). They are in fault contact with the Nakanotake metagabbroic mass on the south, Cretaceous to Paleogene granitic rocks on the north and non-metamorphic sediments of the Ashio Belt on the west (Fig. 4).

The metamorphic rocks can be divided into two units on the basis of lithology of their source rocks and kinds of exotic blocks, that is the A Unit consisting of pelitic banded rock including exotic blocks and B Unit consisting of pelitic rock intercalated with sandstone and conglomerate, including chert blocks. Furthermore, the A Unit can be divided into two lithologic units, the A1 Subunit including metabasalt, metagabbro and ultrabasic rock blocks and A2 Subunit including metabasalt, chert and sandstone blocks. The A Unit occupies largely the distribution area of the metamorphic rocks and B Unit is in the axial part of the syncline and in the eastern area.

2. Kawaba metamorphic rocks

According to Takenouchi and Takahashi (2002), source rocks of the Kawaba metamorphic rocks are subdivided into pelitic rocks including exotic blocks of greenstone, limestone, chert and sandstone, and basic rocks consisting of basalt, dolerite, gabbro and tuffs, whose schistosities show a N-S strike and west-dip (Fig. 6). Northwest-trending serpentinite cuts into the schists. The serpentinite includes blocks of schists at map scale (Fig. 6a) and at outcrop scale in a quarry northeast of Taro (Fig. 6b). Blocks of high-grade metamorphic rocks such as high-pressure schist, jadeitite and garnet amphibolite recognized in the Hida Marginal Belt were not found in the serpentinite of this area. The serpentinite in the Kawaba area cuts all the deformed

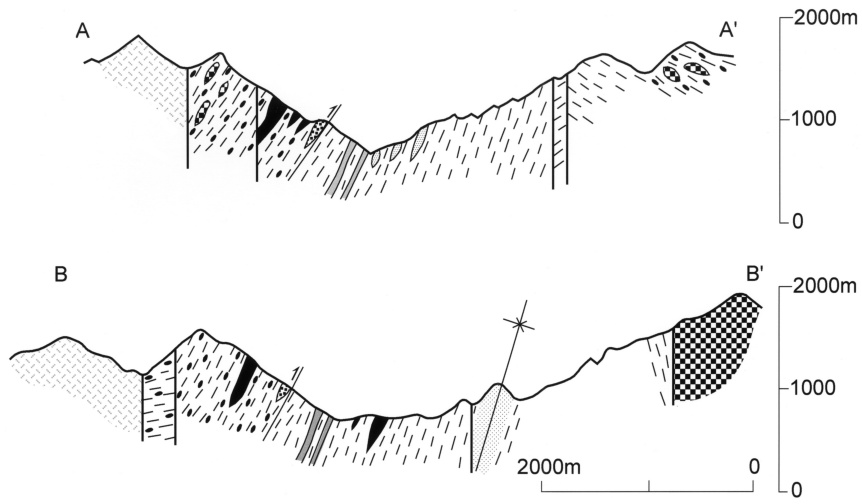

Fig. 5. Geological profiles of the Mizunashigawa metamorphic rocks (modified after Takenouchi, 1988). Profile lines are referred to Fig. 4.

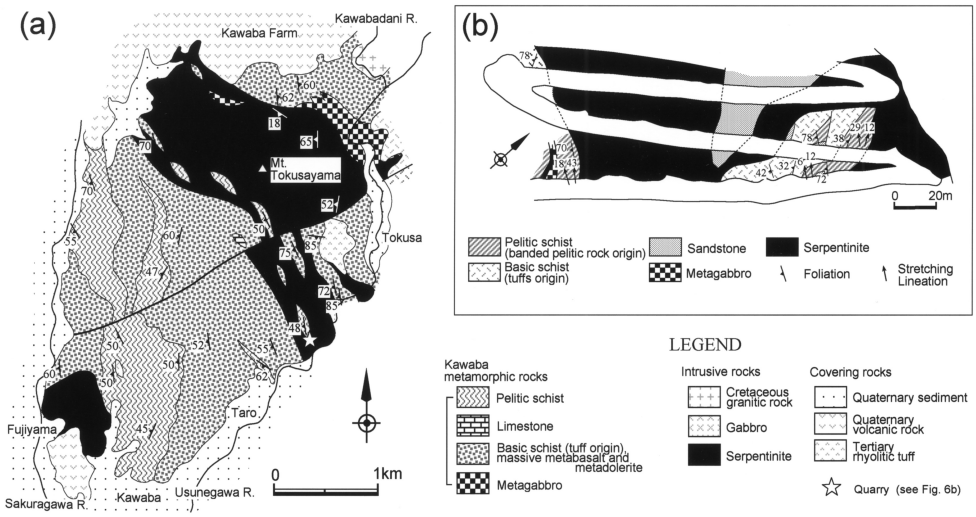

Fig. 6. Geological map (a) of the Kawaba metamorphic rocks, and route map (b) showing the occurrence of serpentinite and schists at the quarry of Numata-Saiseki Co. Ltd (after Takenouchi and Takahashi, 2002).

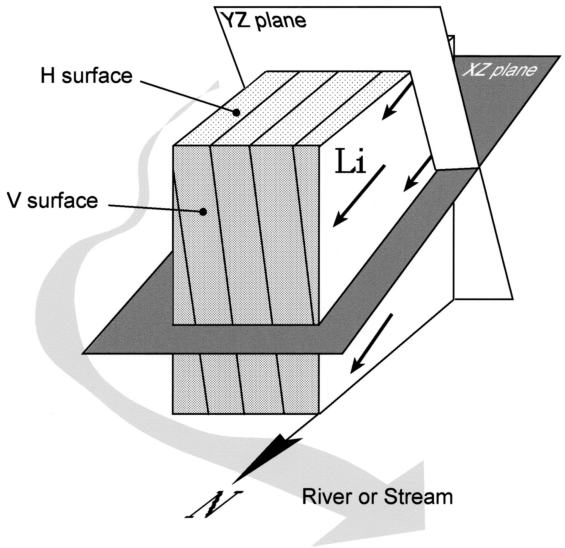

Fig. 7. Figure showing descriptional planes, H and V surfaces, and XZ and YZ planes. Li: Lineation.

minorstructures observed in the schists. The Kawaba metamorphic rocks are intruded by granitic rocks on the northeast and gabbro in the southwest, and covered by Neogene sediments and Quaternary volcanic rocks on the west and north sides, respectively.

The foliation of the basic schists is defined by penetratively developed, deformed thin interbeds of dark green actinolite-rich layers and light green epidote-albite layers in tuffs, and non-penetratively developed, shear planes in metabasalt and metadolerite. The mineral assemblage of actinolite-epidote-chlorite-albite-quartz and actinolite-albite-quartz in the basic schist indicates metamorphism in the greenschist facies.

The foliation of the pelitic schist is defined by penetratively developed, deformed thin interbeds of white quartz-rich layers and brown biotite-rich layers. The mineral assemblage of biotite-muscovite-albite-quartz and chlorite-muscovite-biotite-albite-quartz in the pelitic schist indicates greenschist facies metamorphism.

Structural analyses

1. Mizunashigawa metamorphic rocks

(1) Description of deformed minorstructures

Stretching lineation does not develop penetratively but develops in the axial part of the syncline and its surrounding area in metamorphic rocks. In describing the deformed minor and microstructures observed in metamorphic rocks, the following terms are used. Outcrop surfaces parallel and vertical to the river bed are called the ‘H surface’ and ‘V surface’, respectively, and the plane parallel to the stretching lineation and normal to the foliation is called the ‘XZ plane’. The plane normal to the stretching lineation and the foliation is called the ‘YZ plane’

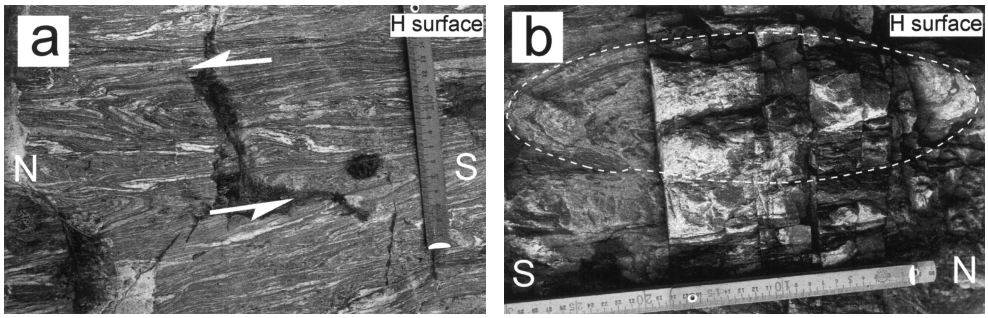

Fig. 8. Occurrence of intrafolial fold and sheath fold. (a) Intrafolial fold showing a left-lateral shear sense on the H surface. (b) Sheath fold showing elliptical YZ cross section on the H surface.

(Fig. 7). The terms, 'lateral' and 'slip' in this paper are equivalent to 'separation' and 'slip' described by Billings (1972).

Intrafolial fold

Intrafolial folds can be observed in siliceous layers and layer-parallel quartz veins. Fold shape is mostly class 1B-2 (Ramsay, 1967) and plane cylindrical with a half wavelength and amplitude of several centimeters. The interlimb angles are 10-60° , which are close to a tight fold. The fold surface in the hinge part bends in a rounded curve or with a sharp angle, such as the chevron type. Shear sense is mostly left-lateral on the H surface (Fig. 8a) and top-to-east on the V surface, and rarely shows reverse sense against the dominant sense in the H surface. Axial plane cleavages without continuous microfolds are rarely observed in the hinge part of intrafolial folds. The intrafolial folds are cut by kink bands. The rootless type of siliceous layer is seen, but is considered to have been formed from lenticular siliceous layers generated by prior non-solid-state deformation.

Sheath fold

The elongated folded layer, like the sheath of a sword, and the long and short axes of the ellipsoid normal to the elongated direction correspond to the X-, Y- and Z-axes of a strain ellipsoid (Henderson, 1981), respectively. Some sheath folds are observed as elliptical folded layers on the H surface at the upper reaches of the Sanashigawa River (Fig. 8b). The ellipsoid, with a long axis 30 cm to 1 m in length and Class 1B-2 in shape, is intrafolial. The directions of the X- and Y-axes are parallel or subparallel to the dip and strike directions of the bedding foliation, respectively. Siliceous layers in the hinge part of the sheath fold form microfolds with weak axial plane cleavage.

Crenulation cleavage

There are two types of crenulation cleavage, i.e., symmetric and asymmetric. Symmetric crenulation cleavage develops at the western side of the axial part of the syncline in the upper

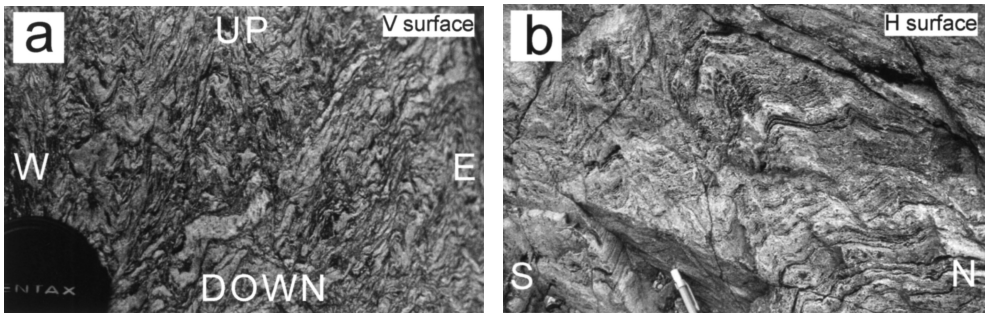

Fig. 9. Occurrence of crenulation cleavages, symmetric (a) and asymmetric (b) types.

reaches of the Mizunashigawa River and the Bunatsurune Stream, whereas the asymmetric type develops in the upper reaches of the Nishifudozawa and Sasabanazawa Streams from the ridge of Mt. Hakkaisan, both of which join the Mizunashigawa River.

Symmetric crenulation cleavages with microfolds are observed at the hinge parts of intrafolial folds, the half wavelength of which is about 5 m, with the horizontal fold axis on the V surface (Fig. 9a). Lithologic facies in which crenulation cleavages develop are fine interbeds of continuous siliceous and pelitic layers. The crenulation cleavage is commonly of the discrete type (Gray, 1977) with the zonal type in local regions without a clear cleavage plane. The cleavage planes are parallel to the axial plane of microfolds with a Class 2 wave shape, a half wavelength of 2-5 cm, and slightly oblique to the general bedding foliation at 10-20°.

The asymmetric crenulation cleavages commonly show zonal type, with local regions of discrete type (Fig. 9b). Symmetric crenulation cleavage is seen at the hinge part of intrafolial folds, whereas the asymmetric crenulation cleavage is seen in general bedding foliation. It is notable that asymmetric crenulation cleavage developed in both lithologies of fine interbeds of siliceous and pelitic thin layers and greenstone mylonite (Fig. 9b). These observations indicate that the asymmetric crenulation cleavages were formed after the formation of greenstone mylonite by shearing.

Drag fault

Drag faults are clearly observed on the H surface. The fault plane strikes nearly E-W and dips vertically. The shear sense along the fault plane shows left-lateral separation judging from the drag of siliceous layers (Fig. 10a). The length of the fault plane ranges from 10-50 cm with displacement of 2-5 cm along the plane. The drag fault cut the mylonite band and is cut by a kink band (Fig. 10b).

In the upper reaches of the Mizunashigawa River, the displacement along the fault plane is

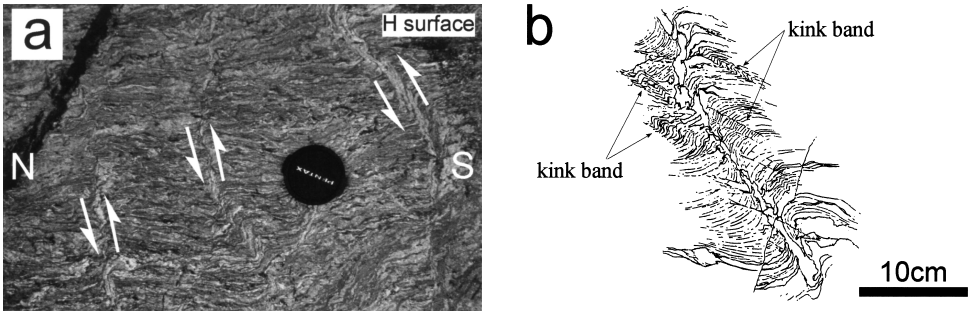

Fig. 10. Occurrence of drag fault (a) showing left-lateral separation on the H surface and sketch (b) showing drag fault cut by kink bands.

about 5 cm and the degree of drag is visible. The degrees of displacement and drag seem to decrease from the upper reaches to the lower reaches of the river.

Kink band

Kink bands are widely developed in the lithology of fine interbeds of siliceous and pelitic thin layers and laminated tuff in the reaches of the Mizunashigawa River. Kink bands are commonly observed on the H surface. According to Uemura and Long (1987), kink bands in general can be classified into four types based on the sense of apparent movement along the kink plane (right-lateral, left-lateral) and the sense of apparent lateral extension or contraction (normal, reverse). The kink bands observed in the rocks are of the following three types (descriptions regarding kink bands follow Uemura and Long, 1987).

Left-lateral reverse type

The hinge part shows angular and rounded wave shapes. Kink planes of some kink bands are visible due to joints along the kink plane. The shape of the kink fold changes in general from an angular hinge, through a rounded hinge, and finally into plane bedding foliation in a manner proportional to increases in the interlimb angle (β). Some kink bands are difficult to discriminate from chevron type intrafolial folds. However, the kink bands could be distinguished from chevron intrafolial folds by the occurrence of long limbs of kink bands coinciding with the bedding foliation and ëchevron intrafolial folds'change their shape to kink bands or conjugate kink bands with increasing interlimb angle. The apparent variety of the interlimb angle is dependent on the angle between the kink axis and outcrop surface.

Right-lateral reverse type

The interlimb angles in the hinge part are larger than those of the left-lateral reverse type. This type is rarely found in the rocks.

Right-lateral normal type

The kink bands show a lenticular shape with visible kink planes and have synthetic

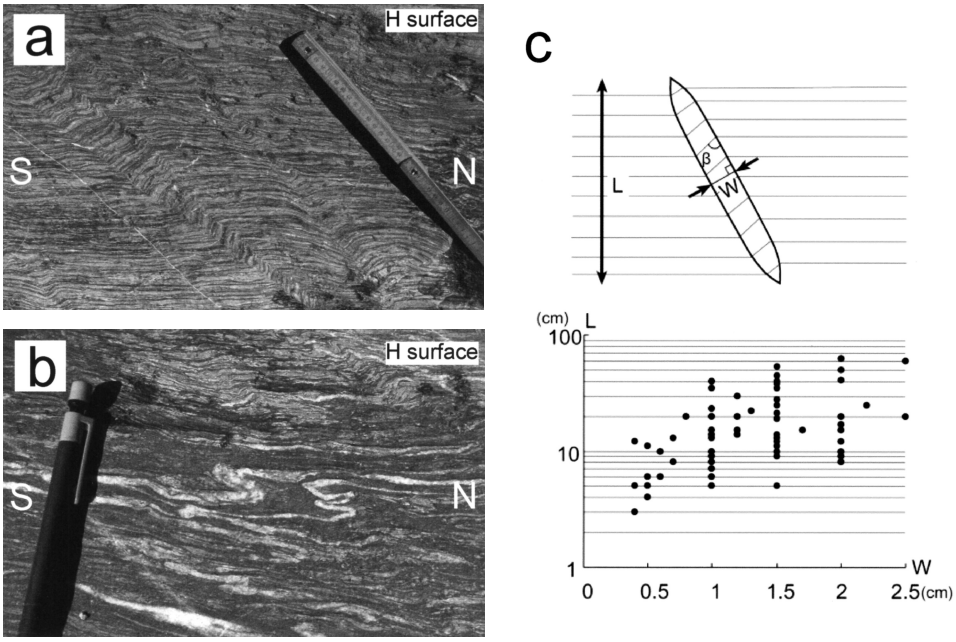

Fig. 11. Occurrence of monoclinal kink bands (a, b), left-lateral reverse type on the H surface, showing a right-lateral shear sense along the bedding foliation, and diagram (c) showing the relationship between length (L) and width (W) of monoclinal kink bands. β shows the angle between short limb within a kink band and kink plane. Note that a kink band cut intrafolial folds of quartz vein (b).

displacement along cleavages parallel to the kink plane at intervals of several mm. A quartz vein along the kink plane is observed in some kink bands.

Mode of arrangement

The mode of arrangement of kink bands is generally monoclinal (Fig. 11a, b), with conjugate and echelon kink bands seen only rarely. Monoclinal and echelon kink bands are of the left-lateral and right-lateral reverse type. Zones in which the monoclinal left-lateral reverse type or right-lateral reverse type develops appear alternately. In addition, zones in which kink bands do and do not develop appear alternately. Asymmetric conjugate kink bands appear in cases in which left-lateral and right-lateral reverse types coexisted within the same zone.

The kink bands are 0.5-2.5 cm in width (W), and are mostly 7-30 cm (maximum 60 cm) in length (L) normal to the bedding foliation consistent with long limb as shown in Fig. 11c.

R_1 Riedel shear

R_1 Riedel shear with synthetic normal displacement develops on the H surface (Fig. 12a) and disturbs the continuous bedding foliation to broken foliation (Figs. 12b, c). This deformation stage shows the first remarkably penetrative brittle regime in the whole deformation process.

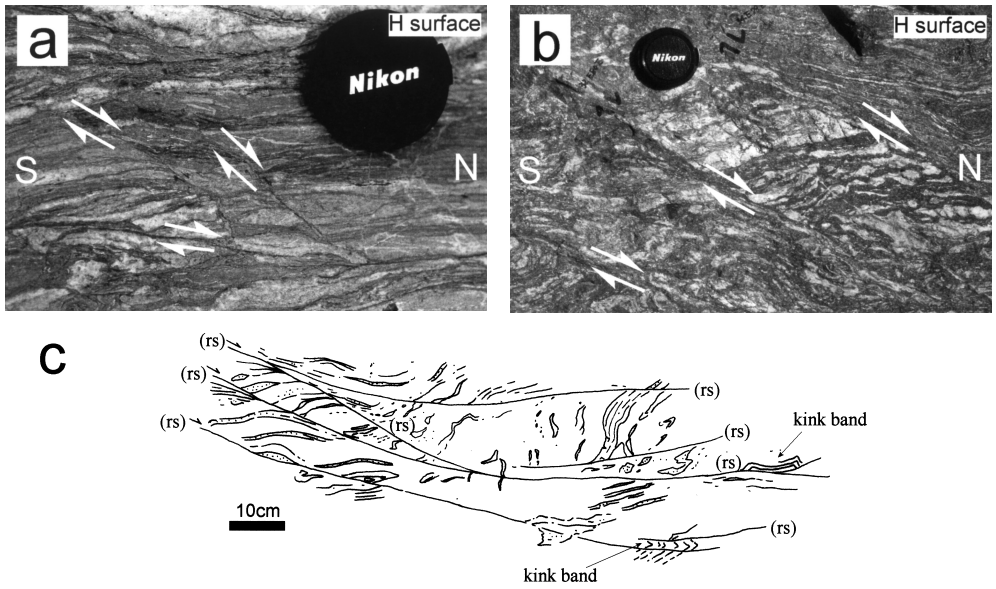

Fig. 12. Occurrence of R_1 Riedel shear (a, b) showing right-lateral shear sense on the H surface. Sketch (c) showing R_1 Riedel shear (rs) cutting kink bands.

The R_1 Riedel shear strikes NNE-SSW and dips steeply at intervals of several tens of centimeters to 1 meter. Displacement along the shear plane (R_1) shows right-lateral separation on the H surface. Y shear is subparallel to parallel to the bedding foliation (Figs. 12a, c). Siliceous layers in the rocks are cut clearly and sharply by the shear planes (R_1 and Y). The R_1 Riedel shear cuts kink bands (Fig. 12c) and is cut by a cataclasite band.

Mylonite band

Mylonite derived from pelitic rocks

Mylonite is defined according to the classification of fault rocks reported by Takagi and Kobayashi (1996). The mylonite bands are recognized as narrow zones, from several centimeters to several meters wide, characterized by intensely stretched siliceous layers and lenses that formed stretching lineations in the rocks. The mylonite bands are parallel to subparallel to the bedding foliation (Figs. 13a, b). Layer-parallel mylonite is observed at the axial part and the eastern side of the major syncline, and the layer-subparallel mylonite is observed at the western limb of the syncline. The layer-parallel mylonite measures from several tens of centimeters up to 5 m in width, while the layer-subparallel mylonite was ten to several tens of centimeters in width (Fig. 13a). The mylonite contains porphyloclasts less than 1 cm in diameter, which made up leucocratic layers in the rocks. The mylonite bands coexist with intrafolial folds, showing no cut-relations (Fig. 13d), and is cut by a drag fault (Fig. 13a).

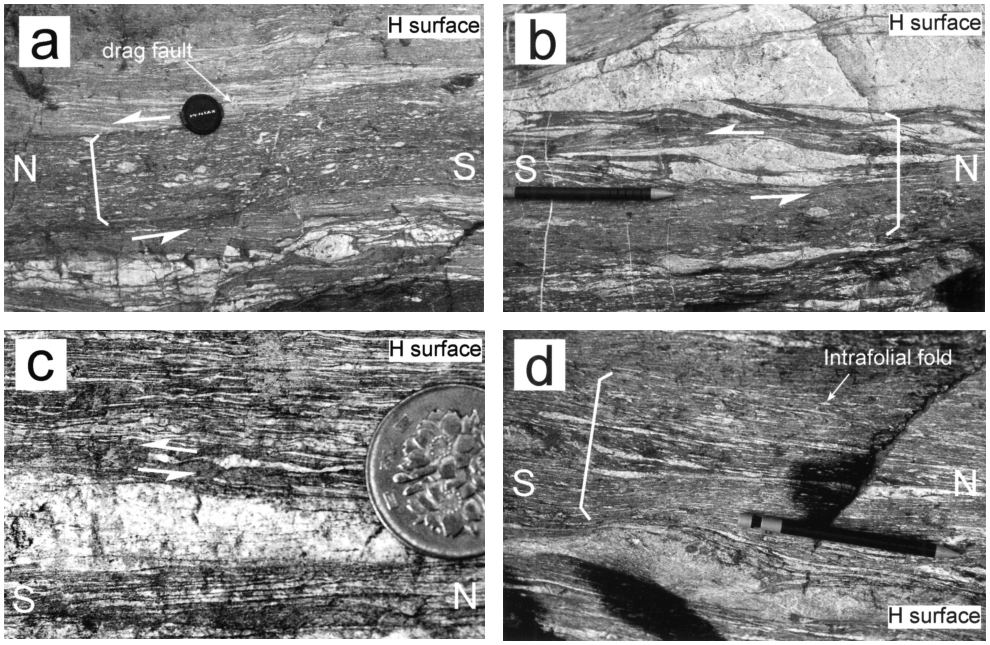

Fig. 13. Occurrence of mylonite bands showing left-lateral shear sense on the H surface. (a) Mylonite band developed in narrow zone slightly oblique to the bedding foliation, and a drag fault cut the mylonite band. (b) Asymmetric elongated sandstone clast in mylonite band. (c) C' type shear band in elongated continuous siliceous layers. (d) Intrafolial fold coexistent with mylonite band.

Asymmetric structures such as the C' type shear band (Fig. 13c), elongated sandstone clast (Fig. 13b), and pressure shadows around porphyloclasts (Fig. 13a) in the mylonite band show left-lateral shear sense on the H surface. By microscopy, deformed structures including the intrafolial folds of quartz veins and rotated porphyloclasts show dominant left-lateral shear sense on the H surface and top-to-east shear sense on the V surface. Muscovite in the mylonite has the following two shapes: 1) muscovite clots 200-400 μm in diameter, and 2) strongly elongated muscovite parallel to the bedding foliation. The strongly elongated muscovite is visible on the H surface.

Mylonite derived from greenstone

The mylonite with mylonitic foliation parallel to the bedding foliation of the rocks develops in greenstone, in the middle reaches of the Nishifudozawa Stream, considered to be an exotic block of the A2 Subunit. The degree of mylonitic foliation development become weak from the basal to the upper part of the greenstone, and finally into massive greenstone.

Asymmetric crenulation cleavages are developed in the mylonitic foliation. Under the microscope, the mylonitic foliation is defined as compositional bands consisting of fine-grained plagioclase layers and blue-green amphibole layers. The mylonite contains lenticular

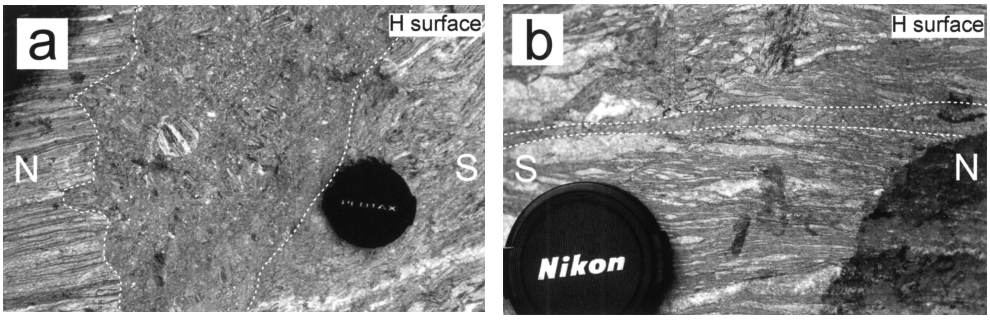

Fig. 14. Occurrence of cataclasite bands showing layer-obilique (a) and layer-subparallel (b) cataclasite bands cutting all deformed minorstructures.

porphyloclasts of coarse-grained hornblende and plagioclase, and C' type shear bands indicating left-lateral shear on the XZ surface (Fig. 18d).

Cataclasite band

Cataclasite is defined according to the classification of fault rocks reported by Takagi and Kobayashi (1996). The cataclasite contains porphyloclasts consisting of rocks less than 1 cm in diameter and angular in shape. The cataclasite have undulatory foliation in the fine matrix, branches and joins in some places, and was 1-15 cm in width (Figs. 14a, b). The relationship between the cataclasite band and bedding foliation is mostly oblique at high angles and the boundary planes of both sides of the cataclasite band are clear and sharp (Fig. 14a).

By microscopy, no syntectonic deformed microstructures can be observed because their structures had disappeared due to newly formed very fine-grained biotite as a result of contact metamorphism (Fig. 18c). The cataclasite band cut all of the deformed minorstructures described above.

(2) Sense of movement and deformation mechanism

Intrafolial fold

The fabrics of the intrafolial folds are shown in Fig. 15b. Intrafolial folds are considered to have formed by so-called drag caused by foliation-parallel shear. The left-lateral shear sense on the H surface and top-to-east sense on the V surface from the drag of folded layers shows relatively south-upward-directed movement of the hanging wall. The shear senses of the intrafolial fold and mylonite bands and attitude of the stretching lineation are shown in Fig. 16. Notably, the shear senses in both limbs of the syncline are the same, indicating that the intrafolial fold, mylonite bands, and stretching lineation were formed after completion of the isoclinal syncline.

Sheath folds

Sheath folds can be formed under a strong shear regime (Minnigh, 1979; Cobbold and

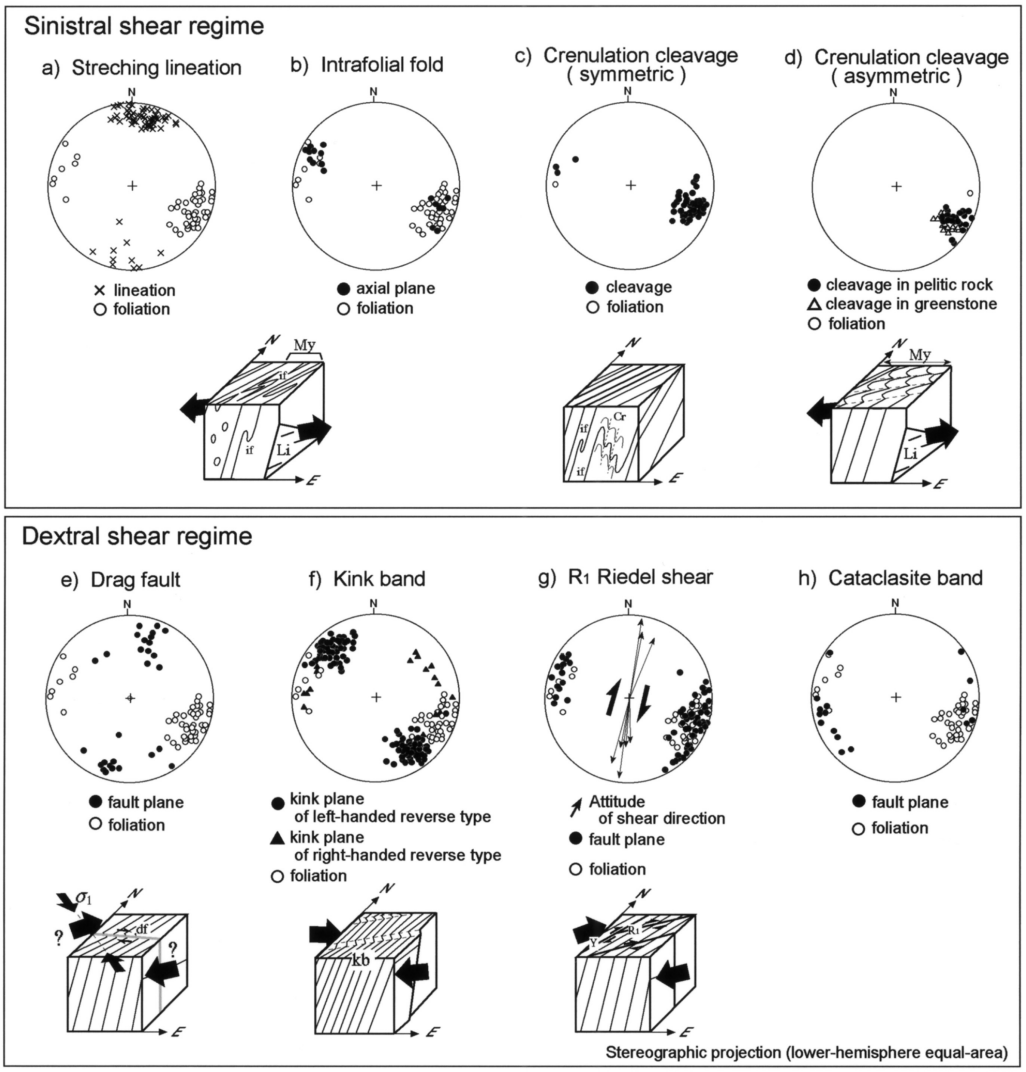

Fig. 15. Fabrics and relative movements of deformed minorstructures in the Mizunashigawa metamorphic rocks.

Quinquis, 1980). The sheath folds in the Mizunashigawa metamorphic rocks were formed by strong shear parallel to the dip-direction of the bedding foliation. Subsequently, microfolds with weak axial plane cleavages in the hinge part were formed by contraction normal to the bedding foliation.

Crenulation cleavage

Crenulation cleavage with symmetric microfolds in the hinge part of an intrafolial fold is considered to be formed by layer-parallel compression after formation of the intrafolial fold (Fig. 15c).

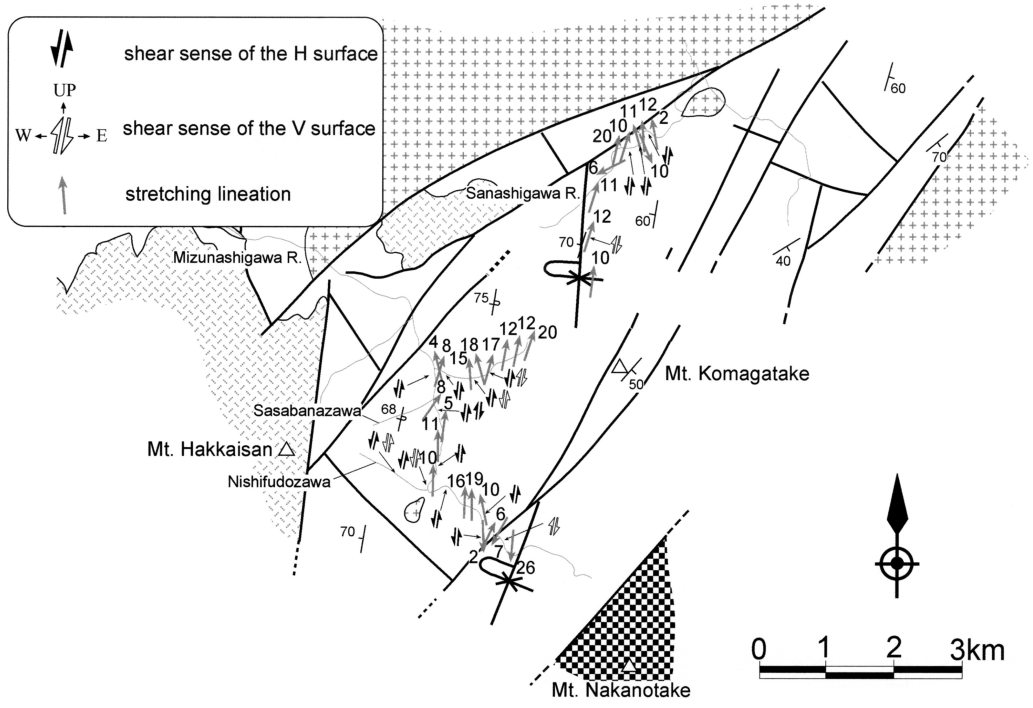

Fig. 16. Map showing the shear sense of intrafolial folds and mylonite bands, and attitude of stretching lineations of siliceous layer. Left-lateral shear sense on the H surface in both eastern and western limbs of a syncline indicates the formation of these structures after completion of the syncline growth. Geological legend is same as those in Fig. 4.

Crenulation cleavage with asymmetric microfolds is considered to be formed by sinistral shear parallel to the bedding foliation judging from the fabrics of the cleavage planes (Fig. 15d).

Drag fault

The fault plane has E-W strike and steep dip (Fig. 15e). The sense along the fault plane shows left-lateral separation on the H surface. However, net slip may have a vertical component on the fault plane. The shear direction on the fault plane could not be identified because it was not possible to observe lineation on the fault plane, which was healed by Cretaceous granitic thermal metamorphism. Therefore, it is impossible to determine the true shear sense and mechanism from the data obtained.

Kink bands

Uemura and Long (1987) showed that monoclinal kink bands and drag folds are formed under different stress fields based on the results of observational, experimental, and theoretical studies of kink bands reported by Dewey (1965), Johnson (1977), etc., and they recommended paying particular attention to discrimination between monoclinal kink bands and drag folds in

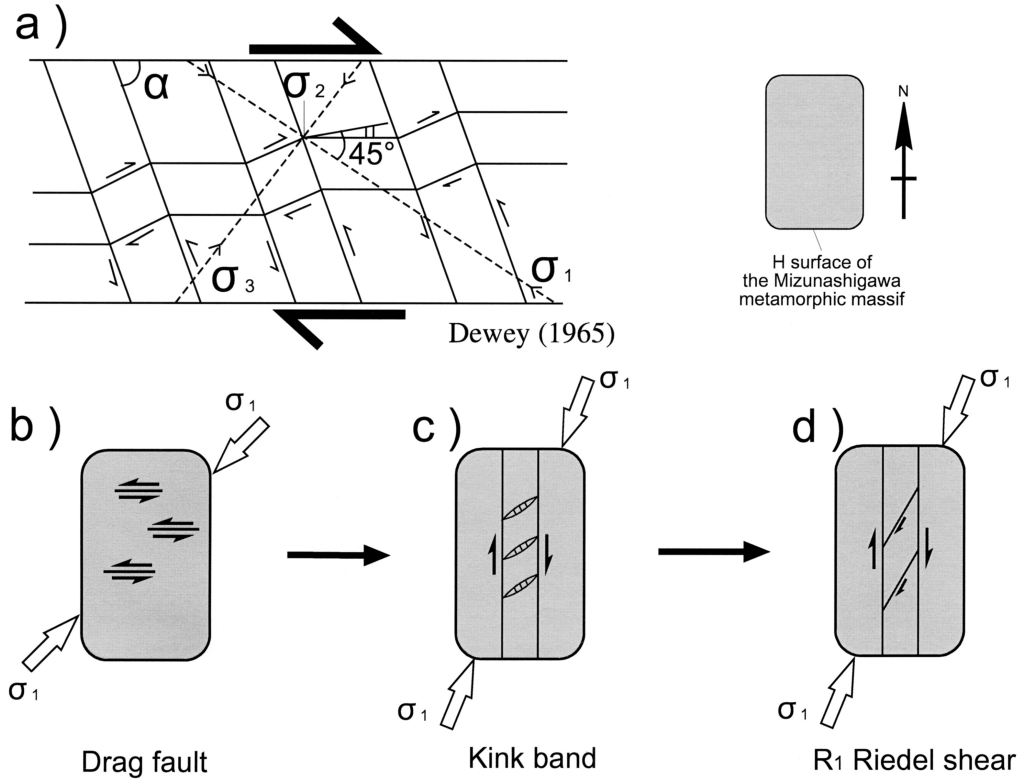

Fig. 17. (a) Relationship between orientation of monoclinal kink bands and stress field (Dewey, 1965). (b)-(d) Relationship between stress field and formation of drag fault (b), kink band (c) and (d) R_1 Riedel shear.

the field (Fig. 15f). The occurrence of monoclinal kink bands indicates that maximum compressive principal stress (σ_1) is oblique to the bedding foliation, *i.e.*, shear stress parallel to the bedding foliation. According to Dewey (1965, Fig. 17a), kink bands were formed under a stress field whose maximum compressive principal stress is in NNE-SSW direction by dextral shear parallel to the bedding foliation (Fig. 17c).

R_1 Riedel shear

The R_1 Riedel shear was formed by dextral strike-slip movement (Fig. 17d) with brittle fracturing. R_1 and Y planes have nearly NNE-SSW strike and steep dip nearly coincident with the bedding foliation (Fig. 15g). Left-lateral shear sense along these planes leads to dextral shear along the bedding foliation.

Mylonite

Mylonite derived from pelitic rocks

Mylonite bands were formed by shearing parallel to the mylonitic foliation. The

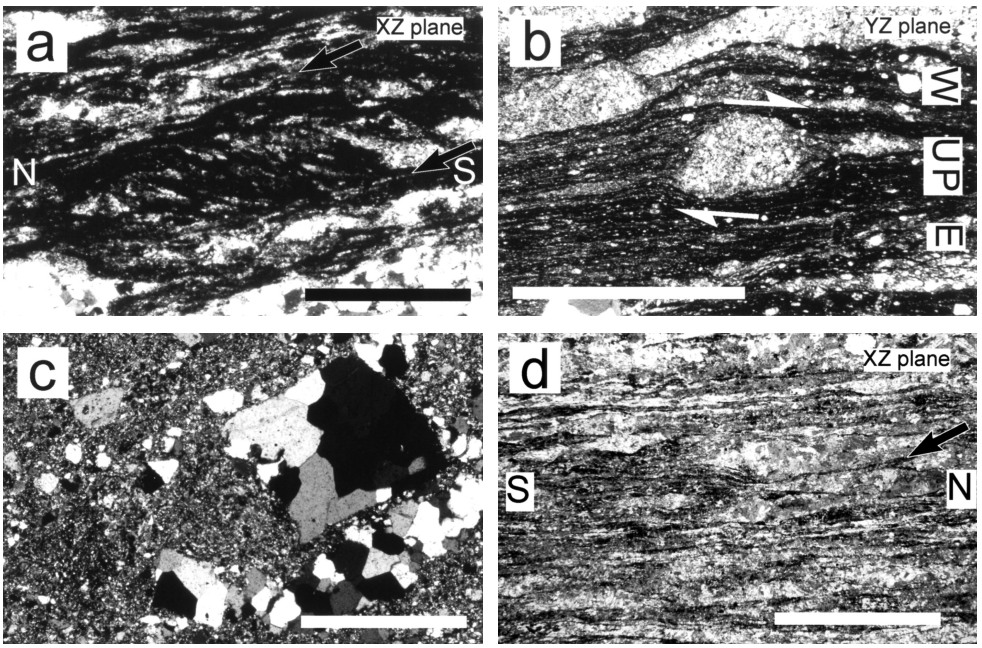

Fig. 18. Photographs of thin sections of mylonite band (a, b), foliated greenstone (d) and cataclasite band (c). Kinematic indicators such as shear bands (C' type, arrows in a, d) and asymmetric (c) pressure shadow (b) show sinistral shear sense on the XZ plane and top-to-east sense on the YZ plane. (c) Cataclasite band including angular porphyloclasts and showing no syntectonic deformed microstructures due to newly formed very fine-grained biotite as a result of contact metamorphism.

asymmetric structures, such as pressure shadow and C' type shear bands, are oriented in a relatively south-upward direction, caused by sinistral-reverse oblique-slip movement of the hanging wall (Figs. 16, 18a, b). The stretching lineation of elongated quartz aggregate and pressure shadow in the mylonite bands suggest that crystal plasticity and diffusive mass transfer have played important roles in the formation of the mylonite bands. Asymmetric structures and strongly elongated muscovites are observed more clearly on the H surface than the V surface. These observations suggest that strike-directed movement was more predominant than dip-directed movement. Elongated muscovite was formed under the regional metamorphism prior to contact metamorphism by granite intrusion because of its syn-kinematic growth.

The coexistence of mylonite and intrafolial folds showing no cut-relation indicates that the mylonite bands were formed at the formation stage of the intrafolial folds.

Mylonite derived from greenstone

C' type shear bands in the mylonite bands show sinistral shear parallel to the mylonitic foliation (Fig. 18d). The textures described previously suggest that the mylonite was derived from greenstone, including hornblende metagabbro.

Cataclasite

Attitude of planes of cataclasite bands is subparallel and oblique to the bedding foliation (Fig. 15h). Cataclasite bands were formed by shearing subparallel and oblique to the bedding foliation. However, the shear sense is not visible because of recrystallization of newly generated biotite by thermal metamorphism due to granitic intrusion.

(3) Deformation facies analysis

Concept of deformation facies

The concept of deformation facies was proposed by Uemura (1981) and can be summarized as follows.

Deformation facies can be defined as characteristics in deformed rocks reflected by the deformation environment and mechanical anisotropy of the rocks. The variety of ductile to brittle deformation styles in rocks is controlled by environment factors and material factors. The former consist of temperature, pressure, time, and derivatives, such as hydrostatic confining pressure, interstitial pore fluid pressure, deviatoric tectonic stress, and their time rates. The latter consist of lithological composition and fabric, such as grain size and its distribution, degree of compaction, mineralogical and chemical compositions, preferred orientation of linear and planar fabric elements, mechanical anisotropy, etc.

For practical purposes, it is useful to represent the environmental and material factors by mean ductility and ductility contrast, respectively. Ductility is defined qualitatively as ductile deformation ability of rocks without fracturing, and quantitatively as the intensity of fracture or yield points in tests of rock mechanical properties. In general, rock is composed of multilayered systems with different ductilities. Ductility contrast shows differences in the ductility of layers, whereas mean ductility shows the mean ductility of the layers. That is, differences in ductility contrast and in mean ductility represent differences in lithology and in deformation grade, respectively. For example, isotropic rocks, such as pure clay stone and limestone, have ductility contrast of ‘zero’, shale is ‘low’, interbeds of sandstone and shale, or fine compositional layers in schists are ‘moderate’, and melange facies of rocks that include rigid blocks or fragments in a ductile matrix are ‘high’. Facies structures are used to identify and correlate the deformation facies. The facies structure includes deformation conditions of environmental factors and material factors.

Based on the concept of deformation facies, deformed minorstructures as facies structures observed in rocks can be arranged systematically on deformation facies diagrams (DFD) represented by mean ductility and ductility contrast as the ordinate and abscissa of a rectilinear coordinate system, respectively. Ductility contrast allows discrimination of the deformation series in a given material, and mean ductility shows the deformation grade for a given material. The above concept of deformation facies allows us to identify, correlate, and zone the deformation facies in nature, and discuss and interpret the mutual relationships between deformation processes and mechanisms (Uemura and Yokota, 1981; Takenouchi, 2000; Takenouchi and Takahashi, 2002; Takenouchi, 2004).

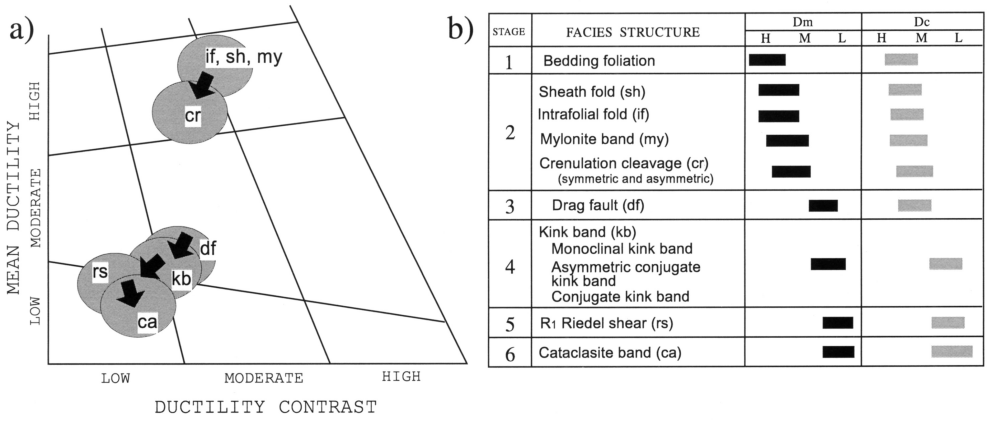

Fig. 19. Deformation facies diagram (a) and deformation stage (b) showing the decreasing of deformation grade with time. Dm: Mean ductility, Dc: Ductility contrast, H: High, M: Moderate, L: Low.

Temporal sequence

The deformed minorstructures developed in the Mizunashigawa metamorphic rocks can be divided into six deformation stages depending on their mutual temporal relationships in the field, *i.e.*, in formative order: 1) bedding foliation, 2) intrafolial fold, sheath fold, mylonite band, crenulation cleavage (symmetric, asymmetric), 3) drag fault, 4) kink band, 5) R_1 Riedel shear, and 6) cataclasite band (Fig. 19b). The relationship between crenulation cleavage and drag fault could not be observed. However, the drag fault is inferred to have been formed after the crenulation cleavage, because, as described previously, symmetric crenulation cleavage was formed synchronously with the intrafolial fold and mylonite band, and asymmetric crenulation cleavage was formed concomitantly with the mylonite band.

These deformed minorstructures plotted on the deformation facies diagram, expressed as mean ductility (Dm) and ductility contrast (Dc), are shown in Fig. 19a. The formative order of the deformed minorstructures indicates the temporal sequence showing that the deformation progressed under decreasing mean ductility with time. Intrafolial fold, sheath fold, and crenulation cleavage are regarded as lying within the domain of High-Dm and Moderate- to High-Dc facies, and drag fault, kink band, and R_1 Riedel shear, within the boundary domain between Moderate-Dm and Moderate-Dc facies, and Low-Dm and Low-Dc facies. Mylonite and cataclasite bands are considered to lie within the domain of High-Dm and High-Dc facies, and Low-Dm and Low-Dc facies, respectively. As stated previously, mean ductility at the formation stage of the mylonite band is regarded as the same as the mean ductility of the intrafolial fold stage. It is important to discriminate the deformation phase as discussed later; deformed minorstructures can be divided into two groups, i.e., a High-Dm group and a Moderate- to Low-Dm group.

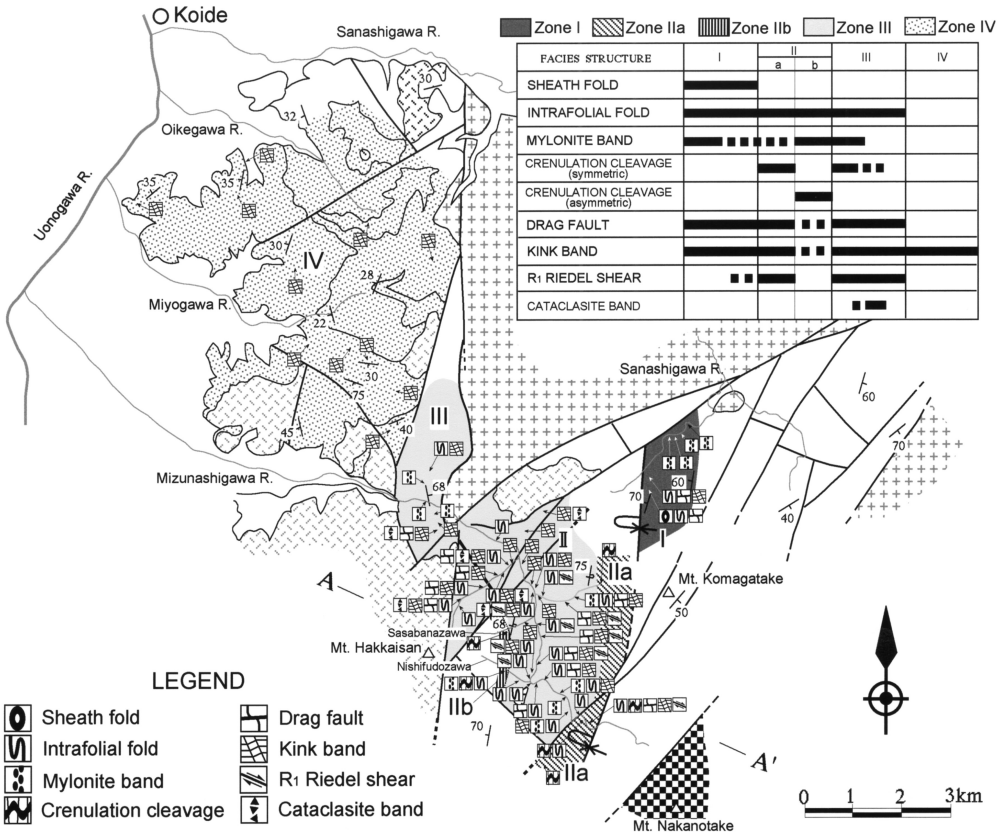

Fig. 20. Table and map showing the deformation zoning based on the assemblage of deformed minorstructures (modified after Takenouchi, 2000). The assemblage of the minorstructures represents change of deformation grade in the zone. Furthermore, the deformation grade decreases with distance from the axial part of a syncline in the western limb. Geological legend is same as those in Fig.4.

Spatial sequence

The spatial development of deformation sequence can be represented by the spatial arrangement of deformation zones (Uemura and Takenouchi, 1984, 1986; Takenouchi, 1985, 1988, 2000; Takenouchi and Takahashi, 2002). Furthermore, the assemblage of the deformed minorstructures also represents changes in the deformation grade in the zones. Deformation grade, expressed by mean ductility shown by assemblages of deformed minorstructures, decreases regularly from zone I and IIa at the axial part of the major syncline, through zone III to zone IV at the western limb of the syncline except zone IIb (Figs. 20 , 21). The development of each deformation zone is not uniform in both limbs, but the decrease in deformation grade in the western limb depends sequentially on the distance from the axial part of the syncline.

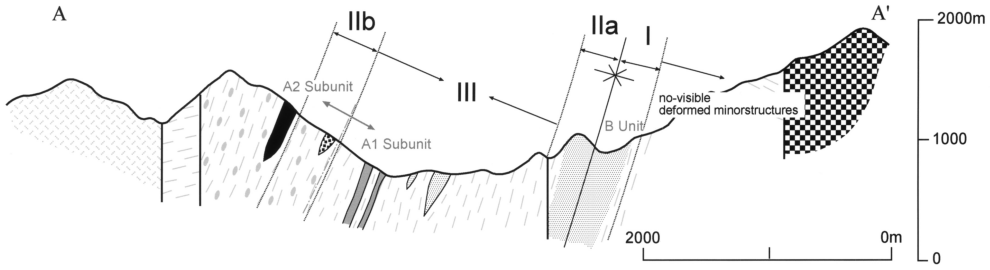

Fig. 21. Map showing deformation zoning profile asymmetrically corresponding to an isoclinal syncline. Geological legend is same as those in Fig.4. Profile line is shown in Fig. 20.

Zone IIb, characterized by asymmetric crenulation cleavage, appears in the boundary zone between the A2 Subunit including ultrabasic rock, metagabbro, and greenstone blocks, and A1 Subunit including chert, sandstone, and greenstone blocks (Takenouchi, 2000; Fig. 22). Asymmetric crenulation cleavage is recognized in both mylonite bands derived from greenstone and pelitic rocks. The formation stage of the asymmetric crenulation cleavage and greenstone mylonite are considered to be the same as those of the mylonite band, intrafolial fold and symmetric crenulation cleavage in pelitic schists.

No visible deformed minorstructures could be observed in the eastern limb out of zone I. This suggested that strain during the deformation process could not be propagated beyond the synclinal axial part to the far eastern region because of E-directed upthrusting of the western massif using mylonite bands in the axial part (Zone I). That is, the temporal and spatial sequences of the deformed minorstructures suggest upthrusting of the Mizunashigawa metamorphic rocks from deeper to shallower levels after formation of the major syncline.

2. Kawaba metamorphic rocks

(1) Description of deformed minorstructures

Deformed minorstructures such as mylonite band, intrafolial folds, crenulation cleavage, drag fault, kink bands, R_1 Riedel shear and cataclasite band occur in the foliation of the schists. The schists locally have a non-penetrative low-angle, NW-plunging stretching lineation defined by alignment of mafic mineral aggregates in the basic schist and elongated quartz aggregates of siliceous layers in the pelitic schist (Fig. 23) on the foliation planes. In contrast, the stretching lineation in a block of basic schist enclosed within serpentinite in northeast of the quarry northeast of Taro plunges at a high-angle.

Mylonite band

Mylonite band is recognized as narrow zones, from several centimeters to meters wide, characterized by intensely stretched siliceous layers and lenses which form stretching lineations in

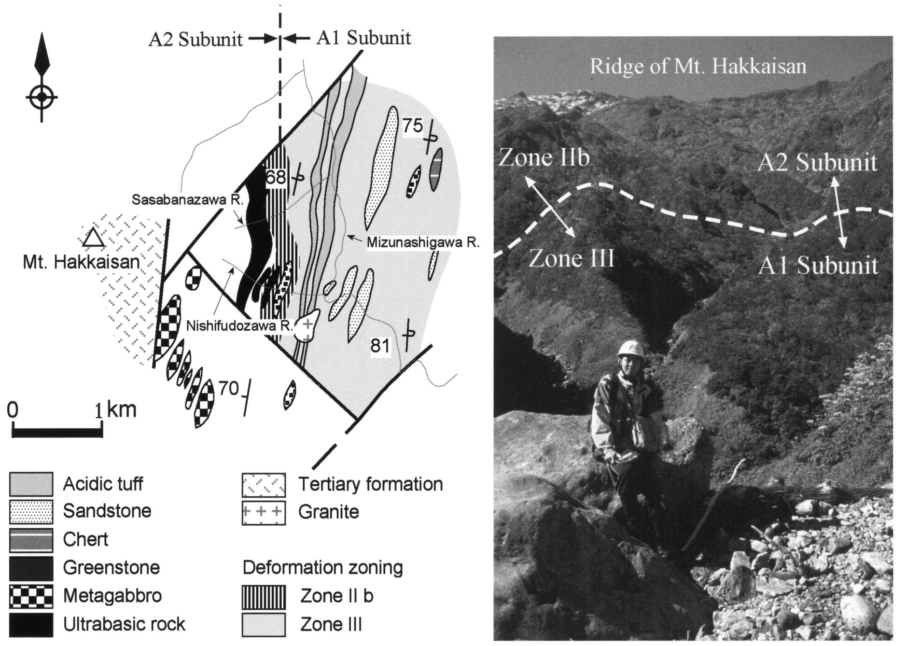

Fig. 22. Map showing the relationship between geology of the Nishifudozawa and Sasabanazawa areas, and distribution of zone IIb of deformation zoning. Zone IIb characterized by deformation structures such as asymmetric crenulation cleavage and greenstone mylonite appears in the boundary area between the A2 Subunit including ultrabasic rock, metagabbro and greenstone blocks and A1 Subunit including chert, sandstone and greenstone blocks.

the pelitic schists (Fig. 23a). The mylonite band is subparallel to parallel to the foliation. The mylonite band contains asymmetric structures such as pressure shadows around porphyroclast, C' type shear band (Passchier and Trouw, 1996; Fig. 23b) and intrafolial fold of stretched siliceous layers on the XZ plane. Dark seams consisting mainly of phyllosilicates are observed on both sides of the siliceous layer in the mylonite band. Layer-normal veins in the siliceous layer are cut along the layer-parallel dark seams. The stretching lineation is overprinted by a subsequent stage of kink band.

Intrafolial fold

Intrafolial fold shows class 2 wave shapes (Ramsay, 1967) whose half wave-length and amplitude are several centimeters, and range from close to tight folds (Fig. 23c). Fold surfaces at the hinge part bending roundly without any minor and micro cleavages, and minor faults can be observed under the microscope. The shape of a dragged layer on the vertical outcrop surface shows relatively eastward directed, thrust component.

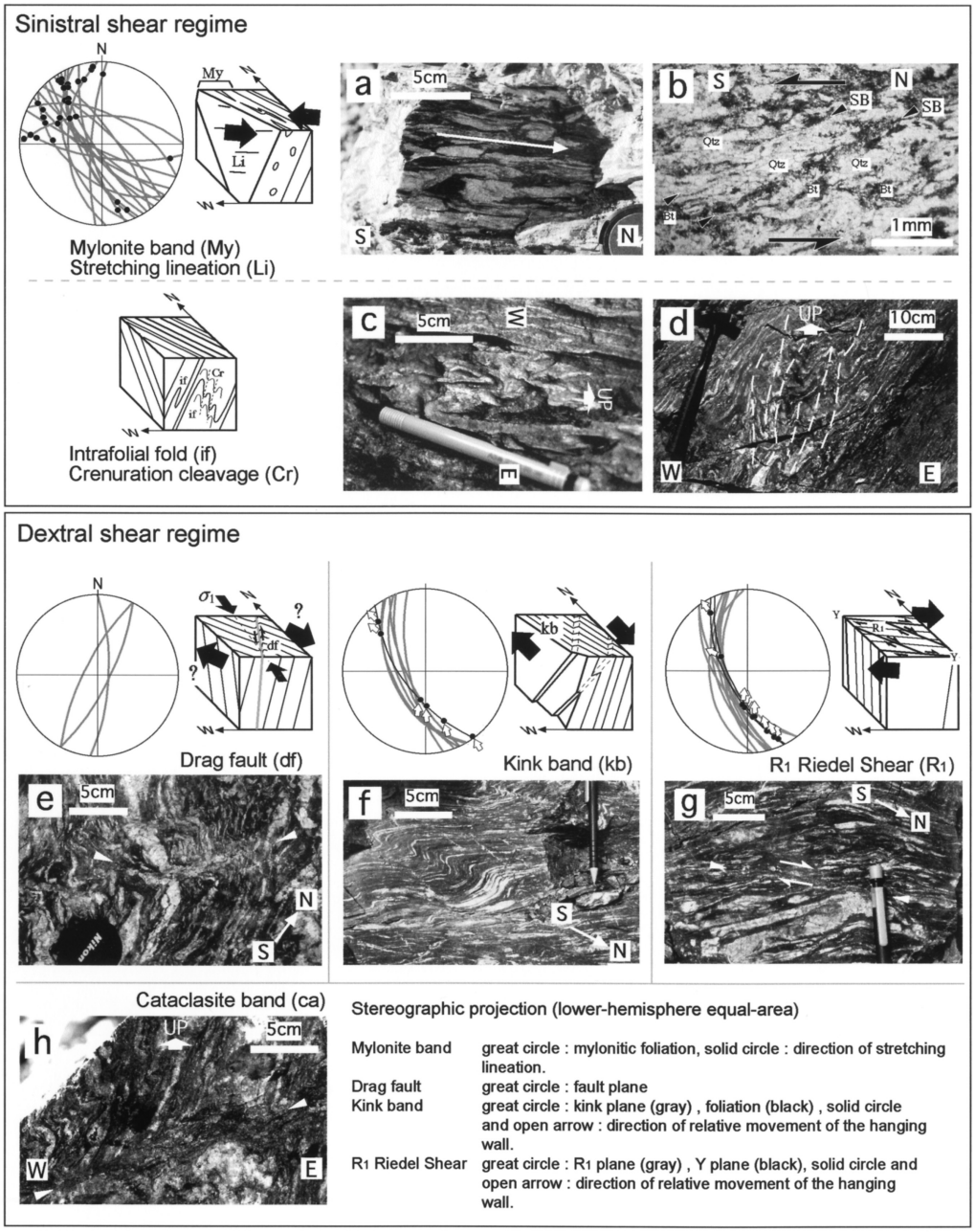

Fig. 23. Occurrence, fabrics and relative movements of deformed minorstructures in the Kawaba metamorphic rocks (after Takenouchi and Takahashi, 2002). (a) Stretching lineations defined by elongated quartz aggregates of siliceous layers with intrafolial folds. (b) Photomicrograph of C' type shear band (SB) on the XZ plane of the mylonite band, showing relatively southward directed, reverse oblique-slip movement. Bt: biotite and Qtz: quartz. Plane polarized light. (c) Intrafolial folds on the V surface showing relatively eastward directed, thrust component. (d) Axial planes (dashed lines) of the crenulation cleavage at the hinge part of an intrafolial fold on the V surface. (e) Drag fault showing a left-lateral separation on the H surface. (f) Monoclinal kink bands, left-lateral reverse type on the H surface, showing dextral shear sense. (g) R_1 Riedel shear on the H surface, showing a dextral shear sense. (h) Cataclasite band on the V surface.

Crenulation cleavage

Asymmetric crenulation cleavage, zonal type (Gray, 1977) without clear discrete cleavage planes, are developed at the hinge part of intrafolial folds with horizontal fold axes (Fig. 23d). The half-wave length of microfolds is several centimeters. The axial planes are oblique to the axial plane of the intrafolial fold and the foliation of the pelitic schist.

Drag fault

Drag fault is a fault having dragged layers, which is observed on the H surface. The fault plane strikes nearly NNE-SSW, and dips steeply. The drag of the layers along the fault plane shows a left-lateral separation (Fig. 23e). The length of the fault plane ranges from 10 to 30 cm and displacement along the plane is less than 3 cm. Siliceous layers of the pelitic schist are dragged, but cut clearly, by the fault plane.

Kink band

Descriptions regarding kink bands follow Uemura and Long (1987). Kink band shows left-lateral reverse type on the H surface. Kink plane strikes NNE-SSW and dips steeply. Arrangement modes of kink bands show mostly monoclinal kink bands (Fig. 23f), and rarely conjugate. The wave shape at the hinge part shows angular and round types. The length of the kink band (length measured at right angles to the foliation) is 10-20 cm. The relationship between limbs of folds and foliation distinguishes kink band from asymmetric crenulation cleavage. The long limbs of the kink band coincide the foliation, but the long limbs of microfolds of the crenulation cleavage do not coincide. Kink bands cut the intrafolial fold.

R_1 Riedel shear

The R_1 Riedel shear strikes NNW-SSE and dips steeply at intervals of 1 to several meters. Displacement along the shear plane (R_1) shows right-lateral separation on the H surface (Fig. 23g). Y shear is subparallel to parallel to the foliation. Siliceous layers of the pelitic schist are dragged, but cut clearly and sharply, by the shear plane (R_1 and Y). Absence of crystal plasticity or diffusive mass transfer in deformation mechanism distinguishes the R_1 Riedel shear from the C' type shear band (Takagi and Kobayashi, 1996).

Cataclasite band

Cataclasite band contains an angular porphyroclast of the pelitic schist with a diameter less than 1 cm (Fig. 23h). The cataclasite band is less than 2 cm wide, and anastomoses in some places. The relation between the foliation and cataclasite band is oblique at high angles. The cataclasite band cuts all deformed minorstructures.

(2) Sense of movement and deformation mechanism

Mylonite band

Mylonite band was formed by shearing parallel to the mylonitic foliation. Shear sense indicators such as C' type shear band and asymmetric pressure shadows show relatively southward directed, sinistral-reverse oblique-slip movement of the hanging wall (Figs. 23a, b). The stretching lineation of elongated quartz aggregate and pressure shadow in the mylonite band suggest that crystal plasticity and diffusive mass transfer have played an important part in the

formation of the mylonite band.

Intrafolial fold-Crenulation cleavage

Intrafolial fold and crenulation cleavage were formed by foliation-parallel shear. The sense of shear is, however, unclear. Smooth folded layers without any cleavages suggest crystal plasticity and diffusive mass transfer in their deformation mechanism (Figs. 23c, d).

Drag fault

Only left-lateral separation along the fault plane can not give net slip of the hanging wall. But, as will be discussed later, the drag fault is inferred to have been formed under a dextral shear regime (Fig. 23e). The deformation mechanism is fracturing.

Kink band

According to the stress field by Dewey (1965), a kink band was formed by a dextral strike-slip movement (Fig. 23f), associated with slips on the foliation and kink plane.

R_1 Riedel shear

The R_1 Riedel shear was formed by a dextral strike-slip movement (Fig. 23g) with brittle fracturing.

Cataclasite band

The slip sense forming the cataclasite band is unclear.

(3) Deformation facies analysis

Temporal sequence

The generation formative order of the deformed minor structures of the Kawaba metamorphic rocks is (1) bedding foliation, (2) mylonite band, intrafolial fold and crenulation cleavage, (3, 4, 5) drag fault, kink band, R_1 Riedel shear (the formative order of these structures occupies from 3rd to 5th, but the exact order is not clear), and (6) cataclasite band based on the temporal relationship observed at outcrops. The temporal relationship between drag fault, kink band and R_1 Riedel shear is unclear.

Fabric, kinematic and deformation facies analyses lead to earlier deformation with high mean ductility formed under the sinistral shear regime and later deformation with low mean ductility formed under dextral shear regime as shown in Fig. 28.

The stretching lineation of the mylonite band in the pelitic schist was formed synchronously with the intrafolial fold and crenulation cleavage, because it is reasonable to consider that layer-parallel flows generated in some layers in the pelitic schist formed synchronously non-penetrative occurrences of the stretching lineation, mylonite band and intrafolial folds with crenulation cleavage.

Drag fault belongs to the later deformation phase together with kink band and R_1 Riedel shear that were formed under a dextral shear regime with low mean ductility, but the relative movement of the hanging wall that formed the drag fault is unclear. The dextral shear regime can form the drag fault with left-lateral separation along the fault plane on the H surface, and that is one possible solution. Thus, the drag fault is inferred to be a product formed under the dextral shear regime.

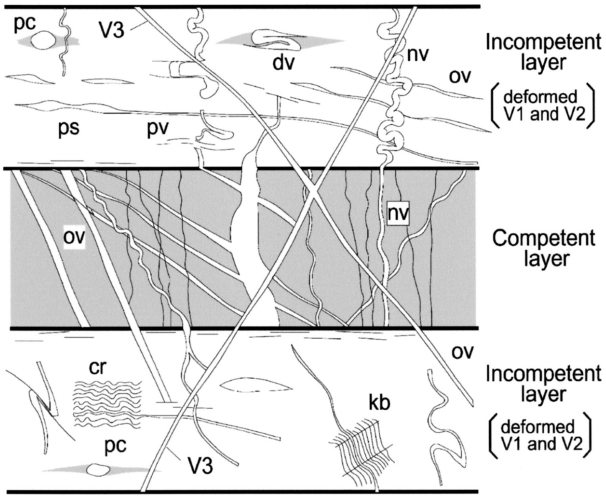

Fig. 24. Schematic deformed microstructures observed in thin sections (after Takenouchi, 2000). ps:pinch-and-swell structures cr: crenulation cleavage, kb:kink band, nv:layer-normal vein, ov:layer-oblique vein, pv:layer-parallel vein, dv:discontinuously deformed vein.

Spatial sequence

Deformation zoning could not be made because of poor outcrops. However, deformation grade in the eastern area is higher than in the western area judging from spatial development of deformed minorstructures.

Tectonic compaction processes from microtextures of deformed quartz veins

1. Description of deformed quartz veins

Variously deformed quartz veins such as folded, stretched and faulted structures can be observed in the low-grade schists consinting of siliceous and pelitic thin layers. The terms of the 'H surface', 'V surface', 'XZ plane' and 'YZ plane' are used here as same as the previous deformed minorstructure descriptions. In description about deformation mode, the terms of the 'competent layer' and 'incompetent layer' are used, whereas about rock origin of layers, the term of the 'siliceous layer', 'sandy layer' and 'pelitic layer' are used, respectively. Deformed microstructures observed in both H and V surfaces are schematically illustrated in Fig.24. Deformed quartz veins in competent and incompetent layers are described separately, because their deformation mode is different.

(1) Quartz vein in competent layer

Layer-normal vein

There are straight and folded quartz veins, which continue through incompetent layers or occur within a competent layer (Figs. 25a, c). In addition, quartz veins in a competent layer which continue through an adjacent incompetent layer and not through another incompetent layer are observed.

Layer-oblique vein

There are straight and folded quartz veins. Straight layer-oblique quartz vein shows at high

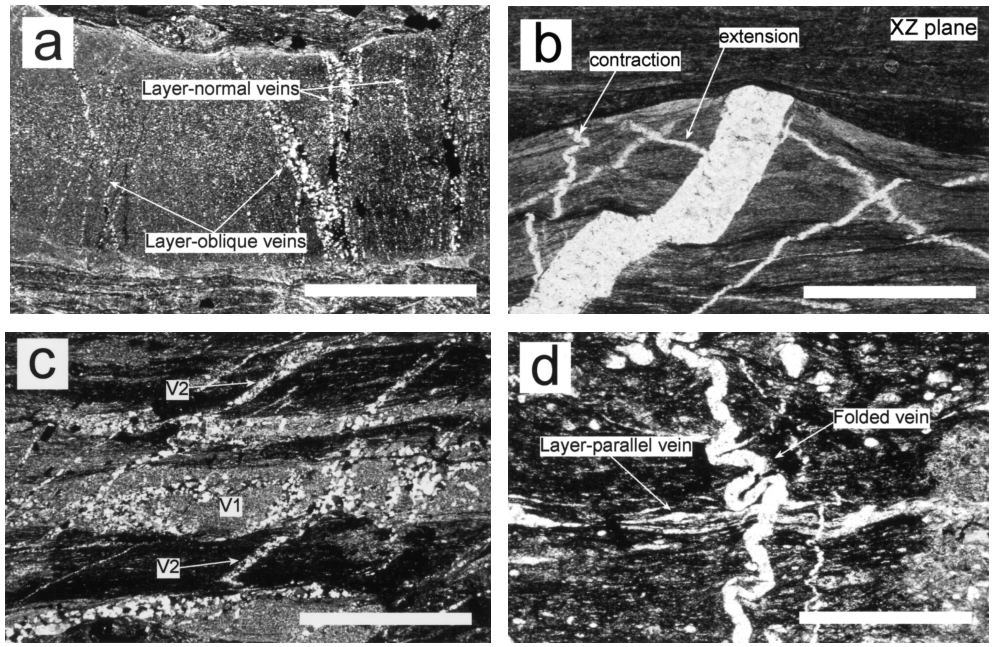

Fig. 25. Photographs of deformed quartz veins. (a) Layer normal and oblique quartz veins (V1) in a competent layer (siliceous layer). Scale bar=2mm, crossed polarizers. (b) Folded and straight quartz veins (deformed V1) in competent layers cut by layer parallel flow in incompetent layers. H surface, Scale bar=1mm, plane polarized light. (c) Layer normal and oblique quartz veins in competent layers (siliceous layer). The veins only in competent layers (V1) and both in competent and incompetent layers (V2) are recognized. V1 veins are cut by layer parallel flow in incompetent layers and thickness of incompetent layers is changed and pinched out. Scale bar=1mm, plane polarized light. (d) Layer normal folded quartz vein (deformed V2) cut layer parallel quartz veins (deformed V1). Scale bar=1mm, plane polarized light.

angles (45-90°) and at low angles (0-45°) to the layers. Their occurrences show that layer-oblique veins continue through both adjacent incompetent layers or through an adjacent incompetent layer and not through another incompetent layer (Figs. 25b, c), and occur only within a competent layer.

Arrangement of high-angled layer-oblique quartz veins shows conjugate (symmetric and asymmetric) and monoclinal. Asymmetric conjugate quartz veins have a folded high-angled vein and another stretched low-angled vein (Fig. 25b). Monoclinal low-angled layer-oblique quartz vein partly converges to both margins of a layer. The mode of quartz vein convergence shows generally left-lateral shear sense and partly right-lateral shear sense on the XZ plane.

(2) Quartz vein in incompetent layer

Layer-oblique vein at high angles (45-90°) to the layers

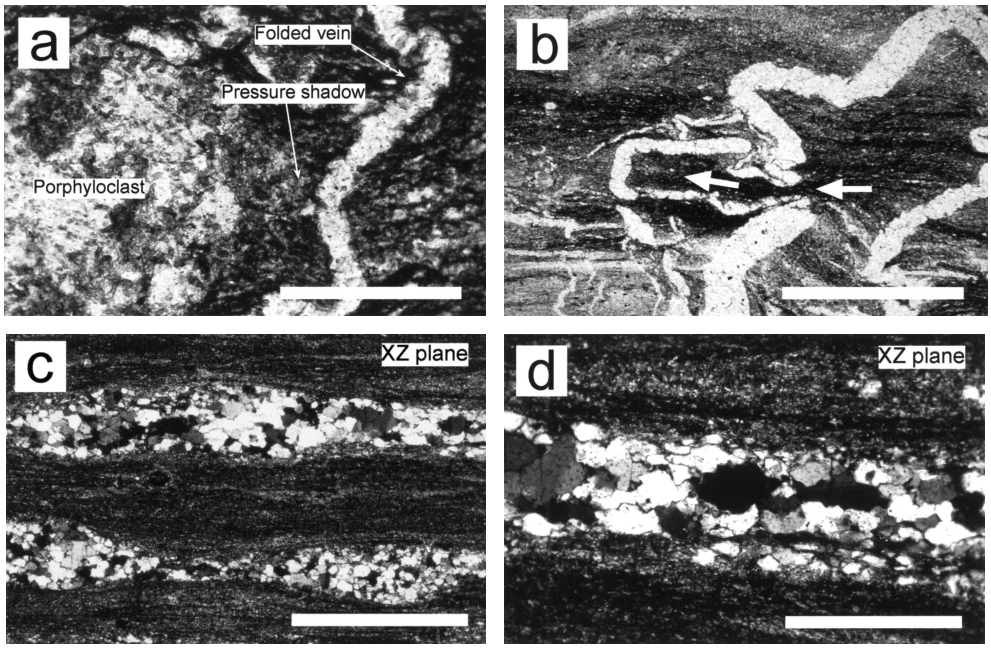

Fig. 26. Photographs of deformed quartz veins. (a) Pressure shadow of sandstone porphyloclast cut by layer normal folded quartz vein. Scale bar=0.3mm, plane plarized light. (b) Layer oblique folded quartz vein deformed by layer parallel flow in incompetent layers. Scale bar=2mm, plane polarized light. (c, d) Pinch-and-swell structure of layer parallel quartz veins having clearly recrystallized grains with irregular boundaries. Scale bar=1mm, clossed polarizers.

There are straight and closely folded quartz veins. Straight quartz vein well continues and commonly passes through incompetent layers. Folded quartz vein shows wave shape varying from Class 1A to 1B (Fig. 25d). In general, Class 1B is predominant in open to closed folds, whereas Class 1A is common in tight to isoclinal folds. The Class 1A folds have irregular half wave-length and amplitude (Fig. 25d). These ptigmatic folds are cut by reverse fault with gap and are displaced by layer-parallel lateral flow (Fig. 26b). In addition, the ptigmatic fold is locally cut away and become into a 'folded mass' which called here the 'discontinuously deformed quartz vein'. High-angled folded quartz vein cut pressure shadows around porphyloclast of fragment (Fig. 26a). High-angled straight quartz vein cut the ptigmatic fold and crenulation cleavage and is cut by a kink band.

Layer-oblique vein at low angles (0-45°) to the layers

There are straight and folded quartz veins. Straight quartz vein partly shows pinch-and-swell structure which continues well or not. In addition, rotated lenticular quartz veins like a boudin structure is observed in part. On the other hand, folds of this type of quartz vein show

open to closed folds, whose interlimb angle is larger than those of high-angled layer-oblique quartz vein.

Low-angled layer-oblique quartz vein is cut by high-angled layer-oblique quartz veins (straight and folded), and cut the discontinuously deformed quartz vein. Furthermore, this type of quartz vein is locally cut away by a small layer-parallel flow and cut by a kink band.

Layer-parallel to subparallel quartz veins occur in only incompetent layers. These veins can be distinguished from sedimentary siliceous layers, because quartz crystals of veins are more large and crystallized than those of the sedimentary layers (Fig. 26d). Layer-parallel quartz vein is narrower in width than other types of quartz vein, and shows boudin, pinch-and-swell structure and intrafolial folds (Class 2 type and rootless type) (Fig. 26c). Recrystallized subgrains of the layer-parallel quartz veins have following characteristics, 1) weak preferred orientation, 2) wavy extinction, 3) irregular boundaries and oblique foliation (Fig. 26d). In some places, layer-oblique quartz vein changes into layer-parallel quartz vein. Layer-parallel quartz vein is cut by crenulation cleavage.

2. Tectonic compaction process

Tectonic compaction process is summarized as shown in Fig. 27.

(1) Deformation process of competent layer

Two formation stages of quartz veins can be recognized from occurrence of the quartz veins passing through incompetent layers or not. The formative and deformative processes of quartz vein in competent layers are considered to be as follows.

(1) Formation of the first quartz vein (V1): Layer-normal and high-angled quartz veins were formed by extension fracture due to layer-normal compression.

(2) Deformation of V1: Layer-parallel shearing added to successive layer-normal compression formed asymmetric conjugate quartz veins, whose two veins were placed in contraction and extension, respectively. Lateral-flow generated in incompetent layers cut the quartz veins which had passed through competent and incompetent layers.

(3) Formation of the second quartz vein (V2): layer-parallel shearing considerably disappeared and then successive layer-normal compression formed V2.

(2) Deformation process of incompetent layer

The formative and deformative processes of quartz veins in incompetent layers are considered to be as follows.

(1) Formation of the first quartz vein (V1): High-angled quartz vein was formed by extension fracture due to layer-normal compression.

(2) Deformation of V1: The former high-angled quartz vein changed into layer-parallel and low-angled layer-oblique quartz veins with rotational structures and discontinuously deformed quartz vein by lateral flow generated by layer-parallel shearing added to successive layer-normal compression.

Asymmetric structures such as rotational structures and intrafolial fold show predominant

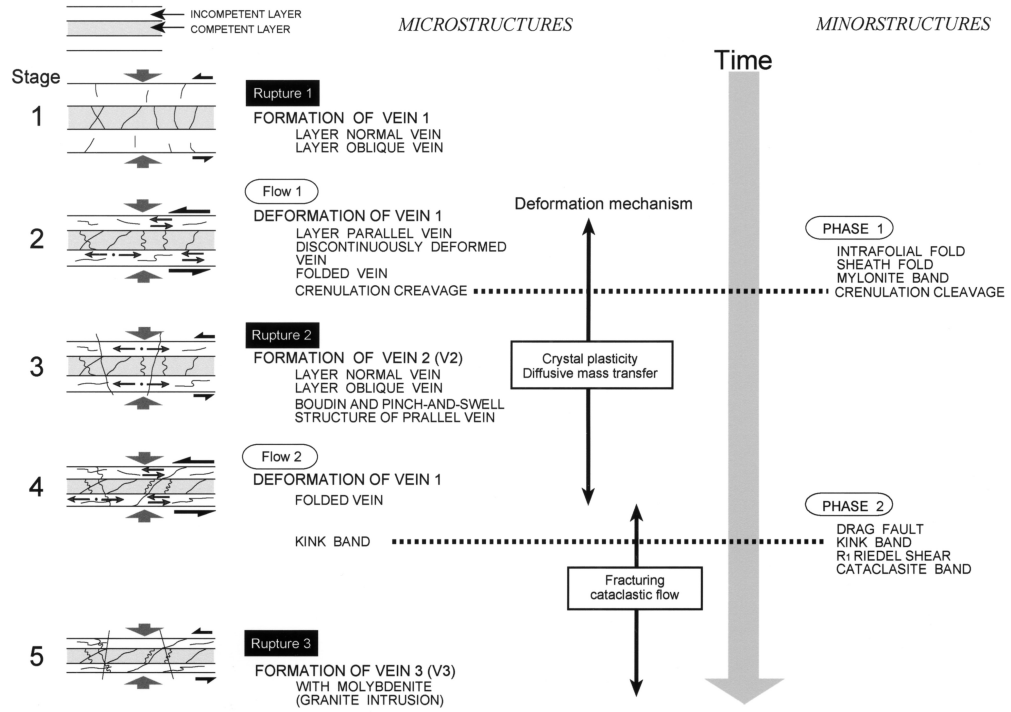

Fig . 27. Formation process of deformed microstructures showing the tectonic compaction of thin bedded competent and incompetent layers (modified after Takenouchi, 2000). Deformation mechanism changed from crystal plasticity and diffusive mass transfer in early stage to fracturing and cataclastic flow in late stage.

left-lateral shear sense, and rare right-lateral shear sense on the H surface. Coexistence of both shear senses indicates that partial bidirected lateral flow resulted from more effective layer-normal compression against layer-parallel shearing (Fig. 27).

(3) Formation of the second quartz vein (V2): Layer-parallel shearing considerably disappeared and then successive layer-normal compression formed V2. Layer-parallel and low-angled quartz veins became to boudin or pinch-and-swell structures with partial rotaion.

(4) Deformation of V2: Layer-parallel shearing added to successive layer-normal compression deformed V2 and previously formed all types of quartz veins.

(5) Formation of the third quartz vein (V3): layer-parallel shearing disappeared and then successive layer-normal compression formed straight quartz vein with molybdenite. Quartz veins in this formation stage are considered to have been resulted from granitic intrusion.

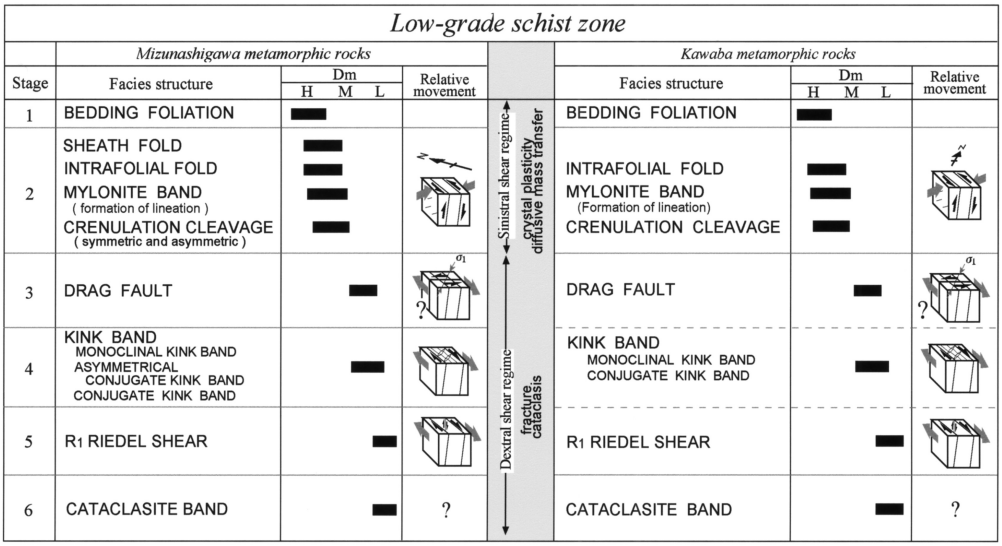

Fig. 28. Deformation stage and relative movement forming deformed minorstructures under two shear regimes in the Kawaba and Mizunashigawa metamorphic rocks (modified after Takenouchi and Takahashi, 2002). Mean ductility of each deformed minorstructures is referred to Uemura (1981). Deformation grade expressed by mean ductility at the formation stage of each deformed minorstructure decreases with time. Dm: Mean ductility, H: High, M: Moderate and L: low.

Discussion

1. Reconstruction of a once continuous low-grade schist zone

(1) Comparison of geology, metamorphism, and deformation history between both low-grade schists

Both low-grade schists have mixed rock facies and diagnostic fine interbeds of siliceous and pelitic thin layers. Furthermore, both low-grade schists show greenschist facies metamorphism. The differences are the large quantities of metabasic rocks in the source rock and wide serpentinite intrusion in the solid state in the Kawaba metamorphic rocks. However, the differences in the source rock between both low-grade schists can be explained by regional differences in spatial development of the accretionary complex. The serpentinite intruded into the Kawaba metamorphic rocks after deformation under a ductile to brittle regime, as stated previously. Therefore, the differences between the two are not essential to discuss continuation.

The formation stage of the deformed minorstructures of the Kawaba metamorphic rocks can be correlated with those of the Mizunashigawa metamorphic rocks as follows (Fig. 28). Intrafolial folds, crenulation cleavage, and mylonite bands of the Kawaba metamorphic rocks can be correlated with the formation stage of sheath folds, intrafolial folds, mylonite bands,

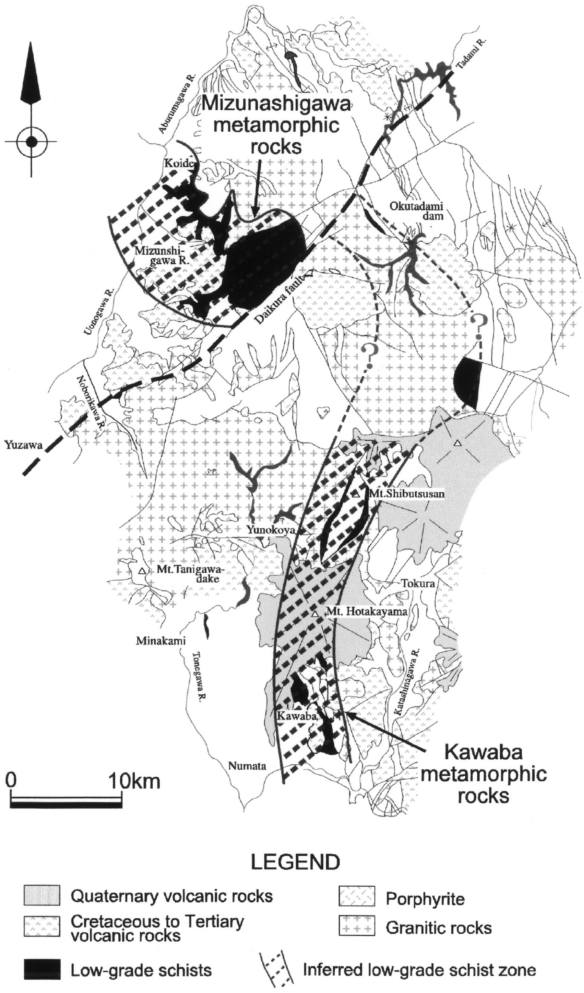

Fig. 29. Map showing distribution of a once continuous low-grade schist zone in the Joetsu region (after Takenouchi and Takahashi, 2002).

and crenulation cleavage in the Mizunashigawa metamorphic rocks judging from the relative movement (sinistral shear) and deformation mechanism (crystal plasticity and diffusive mass transfer) at their formation stages and deformation facies (moderate-high mean ductility and moderate ductility contrast). Although their mutual cut-relations are unclear, drag fault, kink bands, and R_1 Riedel shear of the Kawaba metamorphic rocks were inferred to be correlated with those of the Mizunashigawa metamorphic rocks judging from the relative movement (dextral shear) and deformation mechanism (fracture and cataclasis) at their formation stages and deformation facies (low-moderate mean ductility and moderate ductility contrast). The cataclasite band in the Kawaba metamorphic rocks can be correlated with those in the Mizunashigawa metamorphic rocks because the cataclasite band is the last stage in the deformation history in both rocks. Thus, the Kawaba and Mizunashigawa metamorphic rocks have similar deformation characteristics and history.

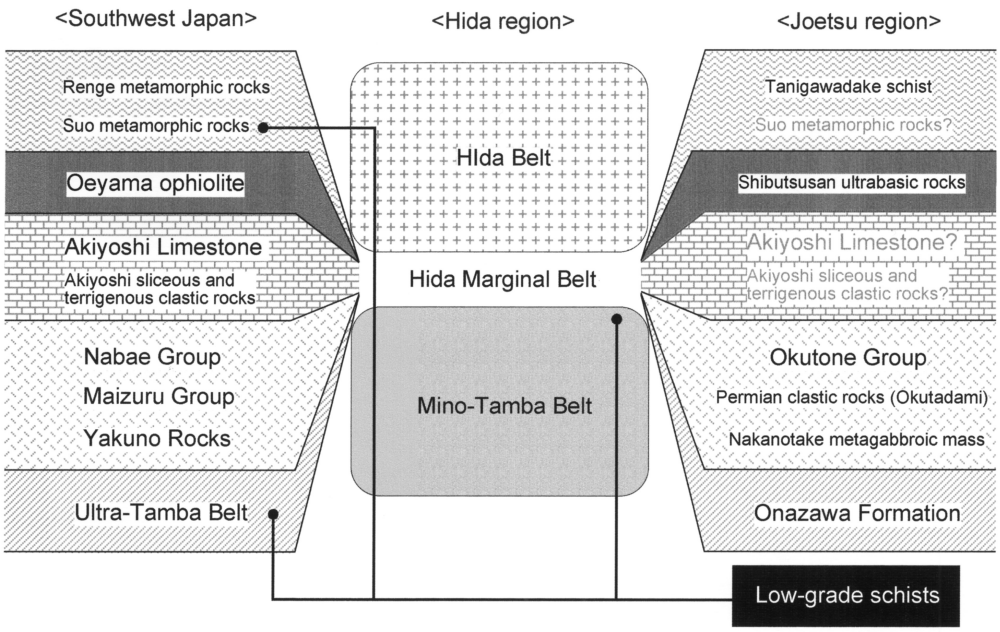

Fig. 30. Correlation between the Inner Zone of Southwest Japan and the Joetsu region.

(2) A reconstructed low-grade schist zone as a key structure to clarify the geology and tectonics of the Joetsu region

Low-grade schists associated with serpentinite of Mt. Shibutsusan are located north of Mt. Hotakayama volcano. The schists are considered to be the northern extension of the Kawaba metamorphic rocks judging from the geological structures (Fig. 29). These schists and the Kawaba and Mizunashigawa metamorphic rocks are regarded as remnants of a once continuous schist zone based on their common constituent rocks, metamorphism, and deformation (occurrence, fabric, assemblage, temporal sequence and deformation mechanism of the deformed minorstructures, and two induced deformation phases). The reconstructed schist zone is a key structure suggesting the structure of the Joetsu region before disturbance of the zonal arrangement by Cretaceous to Neogene crustal movement, plutonism, and volcanism.

(3) Attribution of the low-grade schist

The Paleozoic to Mesozoic systems of the Joestu region have been broadly correlated with the Inner Zone of Southwest Japan. As summarized in Fig. 30, The systems of the Joestu region are considered to be correlated with the surrounding area of the Chugoku-Sangun, Maizuru, Ultra-Tamba, and Tamba Belts on the basis of the constituent rocks, such as Paleozoic high-pressure schists, ultrabasic to metabasic rocks, equivalents of the Maizuru Group, and Ultra-Tamba Belt, Mesozoic shallow marine and brackish water sediments (Upper

Triassic, Lower Jurassic, and Lower Cretaceous), and Mesozoic deep-sea sediments.

However, attribution of the Low-grade schist is vague because of the lack of formation and metamorphic ages. The possible attribution is hypothesized as follows, although the problem must be clarified in future studies.

The first possibility is that it is the equivalent of the Ultra-Tamba Belt. Lithology of the low-grade schist includes diagnostic interbeds of siliceous and pelitic thin layers similar to the UT2 sub-belt (Ishiga, 1986) of the Ultra-Tamba Belt. In addition, Formations of the Ultra-Tamba Belt have intense deformed parts (Caridroit et al., 1985). The low-grade schist tends to appear with Paleozoic ophiolitic rocks like the Ultra-Tamba Belt. On the other hand, formations of the Ultra-Tamba Belt show a common coherent sequence and not mixed rock facies as seen in the low-grade schist in the Joetsu region. Low-grade schist accompanying ophiolitic rocks does not prove its attribution to the Ultra-Tamba Belt, because the Hatto Formation, weakly metamorphosed rocks of Mesozoic deep-sea sediments, is upthrust by ophiolitic rocks (Yakuno rocks), and consequently is adjacent to the ophiolitic rocks in the Mochigase area in Okayama Prefecture (Hayasaka, 1987).

The second possibility is that it is a deformed and weakly metamorphosed part of deep-sea sediments of the Mino-Tamba Terrane, similarly to the Hatto Formation (Hayasaka, 1987) and Unit III of the Kuga Group (Takami et al., 1992). The Hatto Formation includes interbeds of siliceous and pelitic thin layers and shows mixed rock facies including greenstone. In addition, the formation has lineation on the bedding foliation caused by shear deformation (Hayasaka, 1987). Unit III includes thin interbeds of siliceous and pelitic layers and has deformed minorstructures (Takami et al., 1992).

The final possibility is that it is comprised of the Suo metamorphic rocks (Nishimura, 1998) derived from the rocks of the Akiyoshi Belt, a Permian accretionary complex. Any equivalent of the Akiyoshi Belt has not been recognized in the Joetsu region. However, recent geological data suggested the presence of the Akiyoshi Belt in the Joetsu region.

2. Exhumation process of the low-grade schist zone

(1) Deformation history

Progress of tectonic compaction

The formative process of deformed microstructures is summarized in Fig. 27. Layer-normal compression has been working through the whole deformation process and layer-parallel shearings have added to the layer-normal compression at phase 1 and 2 deformations, as discussed later. The deformed microstructures showing shear sense in the twice layer-parallel shearings are more visible on the H surface than the V surface. This indicates that deformation was more intense in the strike-direction than in the dip-direction. Three quartz vein formative stages by extension fracture and two layer-parallel flows during compaction of the rocks were recognized. The compaction of the rocks progressed by staged extension fractures in competent layers and layer-parallel flows in incompetent layers. In conclusion, the compaction was

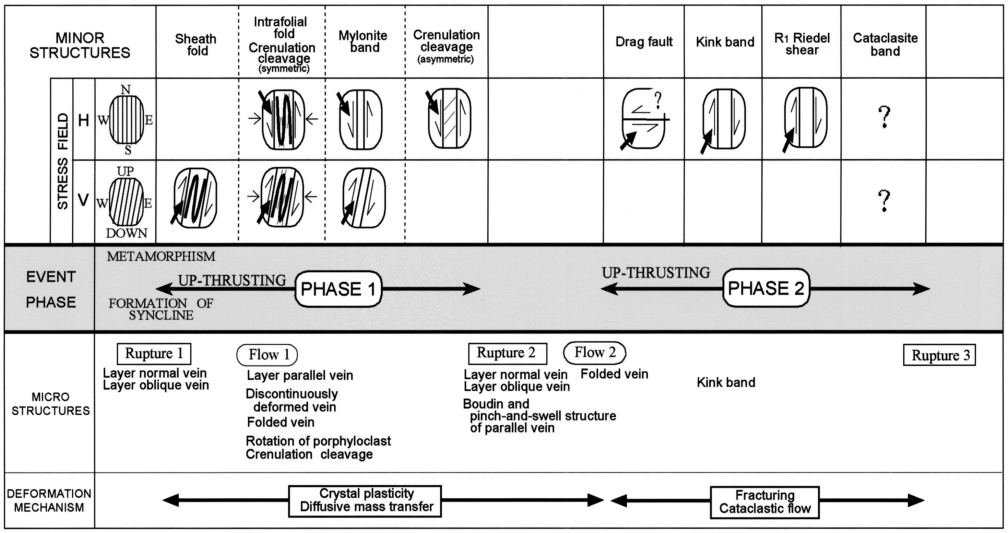

Fig. 31. Deformation history of the Mizunashigawa metamorphic rocks (modified after Takenouchi, 2000). The deformation history indicates two deformation phases which can be elucidated by sheath-intrafolial fold facies to crenulation cleavage facies formed under the sinistral shear regime, and drag fault facies to R_1 Riedel shear facies formed under the dextral shear regime.

considered not only to be sedimentary compaction by burial loading but also tectonic compaction judging from the correlation between deformed minor and microstructures shown in Fig. 27.

Thus, deformed minor and microstructures were formed successively under conditions of decreasing ductility contrast with time in response to progression of tectonic compaction, and under conditions of decreasing mean ductility corresponding to each depth during the exhumation process of the low-grade schist zone from deeper parts, as discussed later.

Change in deformation mechanism

The changes in the deformation mechanism can be summarized as follows.

In the high mean ductility stage, folds, pinch-and-swell structures, and layer-parallel vein of the quartz vein and siliceous layer are considered to have been formed by crystal plasticity based on the following observations. Textures showing dynamic recrystallization (wavy extinction of quartz crystals, oblique foliation of quartz subgrains, and irregular boundaries of quartz subgrains) and absence of any microfaults and cleavages. In addition, diffusive mass transfer was inferred to have played an important role in this deformation stage based on the pressure shadows around the rotation structure of fragments and discontinuously deformed quartz vein, and preferred orientation of phyllosilicates along crenulation cleavages.

In the low mean ductility stage, the deformation mechanism of deformed minorstructures, such as drag faults, kink bands, R_1 Riedel shear, and cataclasite bands, showed fracturing with drag (drag faults), slip consisting of microscopic fracture and cataclastic flow on the foliation and kink plane (kink bands), and cataclastic flow (cataclasite bands).

Thus, the deformation mechanism in the high mean ductility stage shows predominantly crystal plasticity and diffusive mass transfer, whereas those in the low mean ductility stage show predominantly fracturing and cataclastic flow.

Deformation sequence illustrated on the deformation facies diagram

On the deformation facies diagram, with the exception of bedding foliation (stage 1), sheath fold, intrafolial fold, mylonite band, and crenulation cleavage (stage 2) belong to the high mean ductility facies group, and drag fault (stage 3), kink band (stage 4), R_1 Riedel shear (stage 5), and cataclasite band (stage 6) belong to the moderate to low mean ductility facies group. The large difference in mean ductility between both groups can be seen clearly on the deformation facies diagram. This suggested that the whole deformation process consists of two deformation phases, and not a single successive deformation phase.

The shear direction of drag fault (stage 3) is unclear, as mentioned previously. However, the drag fault is inferred to belong to phase 2 deformation as discussed below, because the shear sense of the drag fault shows left-lateral separation on the H surface, which can be explained by dextral shear (Fig. 17b), and the drag fault belongs to the moderate to low mean ductility facies group. In the Mizunashigawa metamorphic rocks, thrust direction of the rocks of the western limb of the syncline, including the axial part, is considered to have changed from south-upward to north-upward at the formation stage of the drag fault. To explain the changes of tectonics and stress fields, it is convenient to consider that NE-SW-directed compression by the north-upward thrusting formed a drag fault with E-W strike and steep dip and subsequent NNE-SSW-directed compression by dextral shear formed the kink band and R_1 Riedel shear (Fig. 17).

Two deformation phases showing inverted shear regimes

Deformation phase can be confirmed by grouping of deformation stages on the basis of formation mechanism, stress field, and deformation facies of deformed minor- and microstructures (Fig. 31).

Deformed minorstructures belonging to the high mean ductility facies were fundamentally formed by upthrusting with a sinistral shear regime having the deformation mechanism of crystal plasticity and diffusive mass transfer. The sheath fold, the x-axis of which was parallel to the dip-direction, is inferred to have developed at the initial stage of upthrusting before sinistral shear. Subsequently, sinistral shear (south-upward-directed shear) formed the intrafolial fold, mylonite band, and crenulation cleavage. These successive deformations explained by upthrusting with sinistral shear are called here ‘phase 1 deformation (earlier deformation phase)’ .

Deformed minorstructures belonging to the low mean ductility facies were formed by

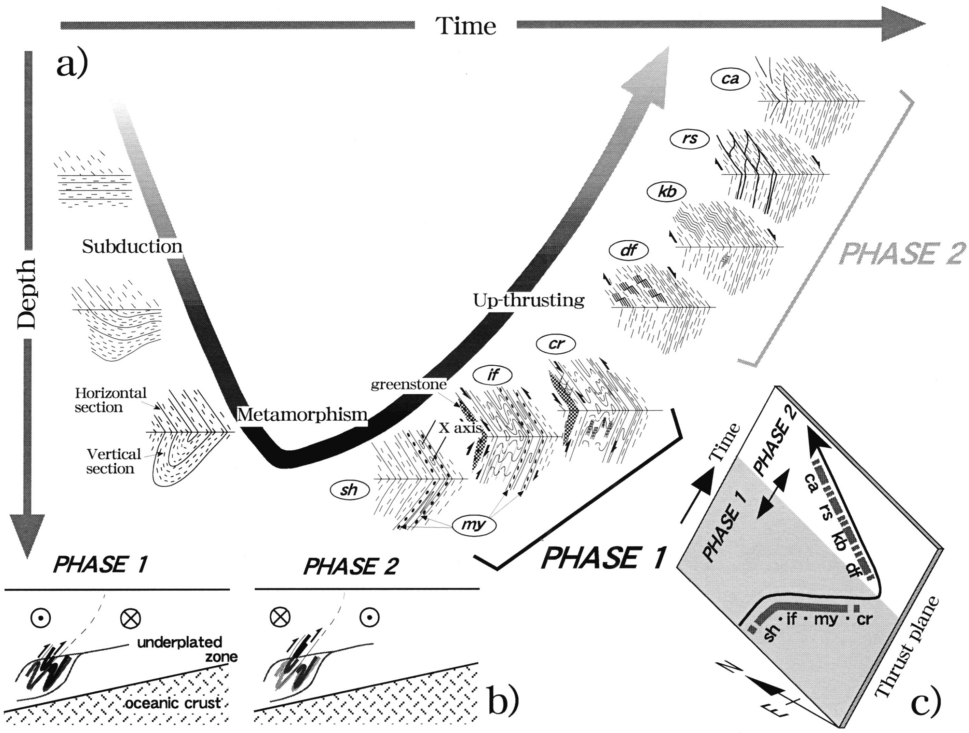

Fig. 32. (a) Kinematic picture of the Mizunashigawa metamorphic rocks from deeper level to shallower one in an accretionary wedge (modified after Takenouchi, 2000). (b) deformation depth in an accretionary wedge at each deformation phases. Circle with dot (cross) indicates movement direction out-of (into) page. (c) Change of movement direction of hanging wall on thrust plane relative to foot wall throughout phase 1 and 2 deformations.

upthrusting with a dextral shear regime, with the deformation mechanisms of fracturing and cataclastic flow. These successive deformations explained by upthrusting with dextral shear are called here 'phase 2 deformation (later deformation phase) '.

(2) Exhumation process

The exhumation process of the low-grade schists is described with the Mizunashigawa metamorphic rocks as an example (Fig. 32).

Formation process of geological structure

Stage A: Formation of the bedding foliation through greenschist facies metamorphism, subsequently formation of the syncline.

Stage B: Mylonite bands were developed in the axial part of the syncline, which resulted from eastward-directed thrusting of the hanging wall of the western limb. Sheath folds were formed by dip-directed intense shear in the footwall synchronously with the mylonite band.

Stage C: Eastward-directed thrusting changed to south-upward-directed oblique-thrusting

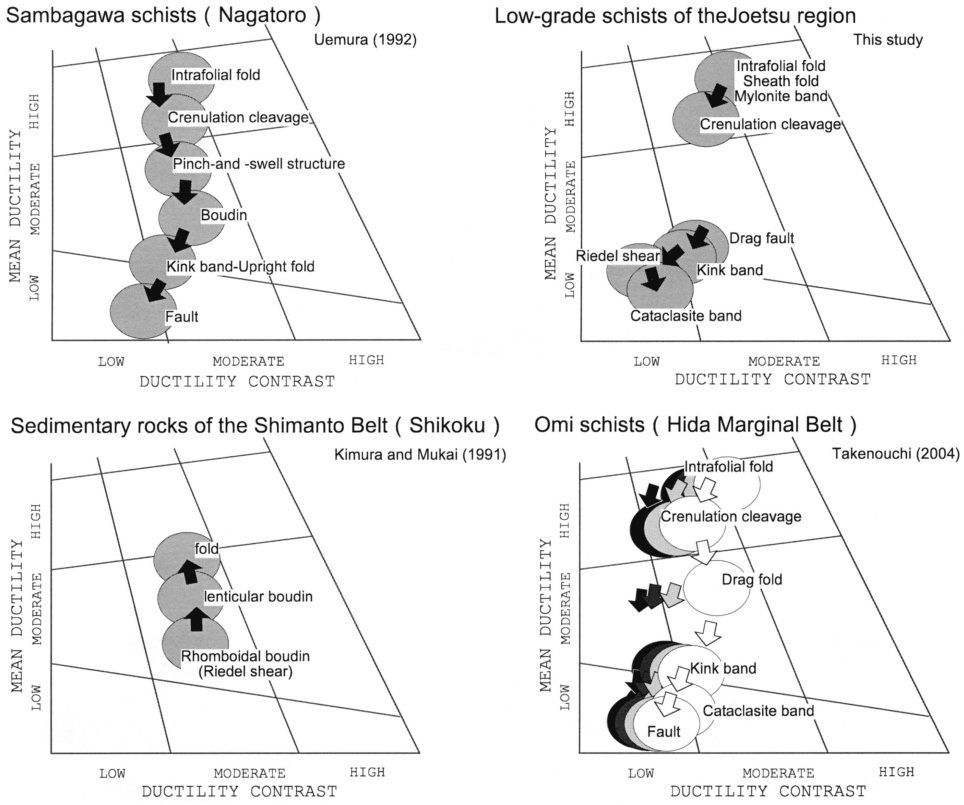

Fig. 33. Deformation facies diagrams showing temporal deformation sequence in some shear belts.

showing sinistral shear. The strain concentrated in pelitic layers of the rocks, because the attitude of the pelitic layers coincided with those of a shear plane of conjugate shear planes with large shear angle under high confining pressure at a deep level. In the strain-concentrated part, mylonite bands, intrafolial folds, and crenulation cleavage were formed. The A2 Subunit including ultrabasic rock, metagabbro, and greenstone blocks has thrust over the A1 Subunit. Consequently, greenstone mylonite and asymmetric crenulation cleavage were formed along the boundary zone between the two units.

Stage D: South-upward-directed oblique-thrusting changed to north-upward-directed oblique-thrusting showing dextral shear. The drag fault was inferred to have been formed at this stage.

Stage E: The kink band was formed by NNE-SSW contraction under a dextral shear regime.

Stage F: R_1 Riedel shear was formed by NNE-SSW contraction under a dextral shear regime.

Stage G: The cataclasite band was formed at a shallower level in the earth's crust.

Temporal deformation sequence of some shear belts

The deformation sequence based on deformation facies analysis was shown to be useful for estimation of the up-lifting process of rock bodies in the Hida Marginal Belt and Hidaka Metamorphic Belt (Uemura, 1984).

The deformation sequence in the low-grade schist of the Joetsu region was described previously. The data discussed in this chapter indicate that geological bodies formed under different tectonic histories, such as the coherent high-pressure schist zone (Sambagawa schists), high-pressure schist blocks in serpentinite melange (Omi schist), and sedimentary rocks of pelitic melange (Shimanto Belt), have individual characteristic deformation sequences. Individual development modes of the deformation sequence in rocks are affected by different deformation environments; consequently this is useful to infer the changes in the deformation environment. The above three deformation sequences are illustrated in the deformation facies diagram in Fig. 33.

Material-circulation in the accretionary complex is considered to occur according to subduction of sediments, their off-scraping and underplating, and then metamorphism in response to their buried depth (Paterson and Sample, 1988). Subsequently, advanced underplating causes thickening and up-lifting of the accretionary complex, and then strike-slip faults and out-of-sequence thrust developing in the accretionary complex accelerate exhumation of underplated materials (Taira et al., 1988; Sample and Moore, 1987). The deformation process from subduction to underplating is represented by a deformation sequence consisting first of rhombic boudin (sheared type), second of lenticular boudin (extension type), and last folding of former boudins in the Shimanto Belt, east Shikoku, as shown by Kimura and Mukai (1991; Fig. 33). This suggested that deformed minorstructures were formed under conditions of increasing mean ductility with time. On the other hand, the deformation sequence in deep-underplated rocks, such as the Sambagawa schist and Omi schist, had been formed under conditions of successively decreasing mean ductility with time during their exhumation process (Uemura et al., 1985; Uemura, 1992; Takenouchi, 2004; Fig. 33).

Thus, the appearance of the deformation sequence on the deformation facies diagram shows a variety of responses to the deformation environment in some shear belts. Especially, the deformation sequence of the low-grade schist is apparently divided into a high mean ductility facies group and a moderate-to-low mean ductility facies group in contrast to the successive deformation sequence of the Sambagawa schist. The deformation sequence of the low-grade schists suggests changes in the stress field, deformation mechanism, and deformation phase. Deformation facies analysis added to classical fabric analysis is a useful tool to reveal unknown tectonics in some shear belts.

If it is possible to recognize the entire deformation sequence of rocks in response to material circulation in an accretionary wedge, it will be possible to obtain two complete deformation sequences on the deformation facies diagram; that is, upward deformation sequence from low mean ductility facies to high mean ductility facies in response to the subduction process, and

downward deformation sequence from high mean ductility facies to low mean ductility facies in response to the exhumation process. However, we cannot commonly distinguish between subduction- and exhumation-related deformation sequences because the latter overprint and erase the former. The distinction could not be made in the present study. Therefore, the deformation sequence recognized in the low-grade schist shows the exhumation-related deformation sequence.

3. Tectonic evolution of the low-grade schist zone

(1) Discussion of the Hida Nappe hypothesis

The 'Hida Nappe hypothesis' was first proposed by Komatsu et al. (1985). The nappe feature was explained by the flower structure model in transpression (Komatsu et al., 1988) or the northward inverted model of thrust duplex by Komatsu et al. (1993). On the other hand, Takagi and Hara (1994) regarded the mylonites developed in the Hida Belt as strike-slip shear zones and not as being of nappe origin.

The kinematic picture of the Hida Belt has been confirmed. However, the Hida Nappe hypothesis was accepted in this study based on the reasons outlined below.

Deformation characteristics of the Hida Marginal Belt

Eastern area

The eastern area occupies the Omi-Range region, on the border of Niigata, Toyama, and Nagano Prefectures, of the Hida Marginal Belt (Komatsu, 1990). Tectonics of the eastern area were proposed by Komatsu et al. (1985) and Komatsu et al. (1993). According to Komatsu et al. (1985), the Hida Nappe hypothesis is based on the following data: 1) N-S trending, east-verging monoclinal structure of the Paleozoic systems, including serpentinite melange, bounded by thrusts, 2) N-S trending sub-horizontal basal serpentinite covers the E-W trending equivalents of non-metamorphosed rocks belonging to the Akiyoshi Belt, and 3) high gravity anomaly beneath the Hida Belt trending in the E-W direction corresponding to the Yakuno ophiolites. Komatsu et al. (1985) regarded the serpentinite melange, including high-pressure schists, garnet-amphibolite, and jadeitite blocks in the eastern area as a footwall, dragged up from a deeper level of the Hida Belt thrusting over the Inner Zone of Southwest Japan.

However, kinematic indicators, such as deformed minor and microstructures suggesting the Hida Nappe, have not yet been reported in this area.

Southern area

The southern area occupies the E-W trending narrow zone characterized by sporadically distributed Lower to Middle Paleozoic systems and high-pressure schist along the southern margin of the Hida Belt.

Otoh et al. (2003) characterized the kinematic direction of this area using deformed minorstructures (Fig. 34). The results can be summarized as follows: 1) Two groups of shear zones, i.e., ductile shear zones formed during the Late Triassic to Late Jurassic, and brittle shear zones formed during the Early to Late Cretaceous, 2) the ductile shear zones show dextral

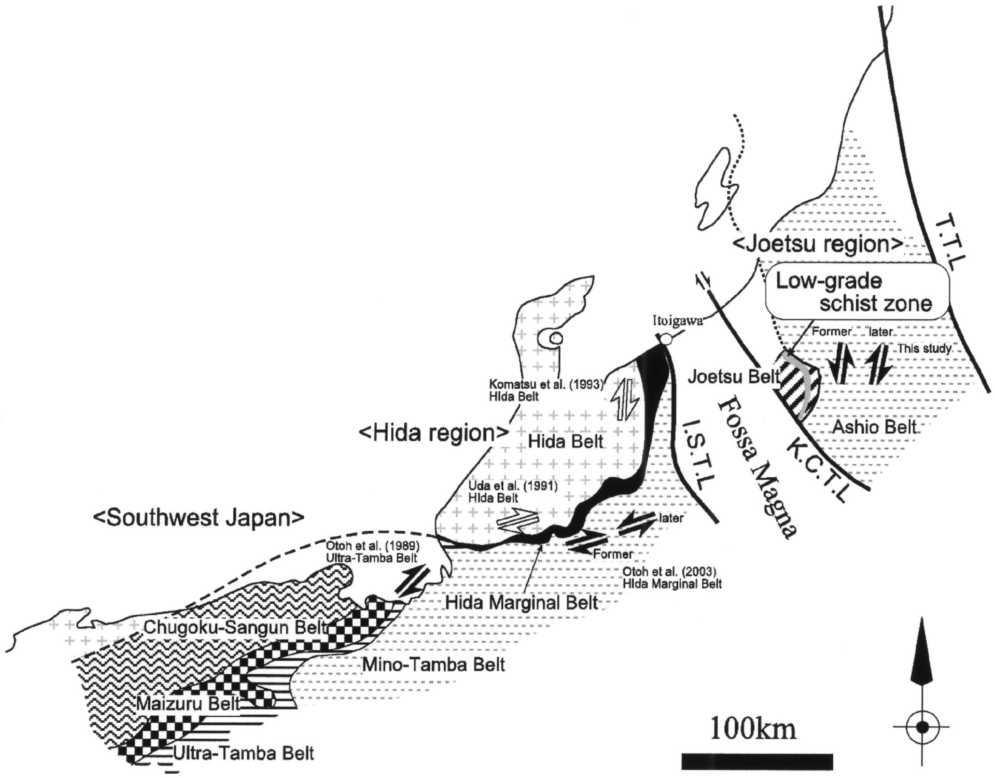

Fig. 34. Map showing shear direction of the Hida Belt and its surrounding area. I.S.T.L: Itoigawa-Shizuoka Tectonic Line, K.C.T.L: Kashiwazaki-Chiba Tectonic Line, T.T.L: Tanagura Tectonic Line. Arrows: lateral shear sense.

strike-slip, whereas the brittle shear zones show sinistral strike-slip, and 3) the ductile shear zones bound sub-belts consisting of the Paleozoic systems.

The above results suggest predominant strike-slip movements in the southern area in contrast to dip-slip movements in the eastern area.

Western area

The western area faces the Wakasa Bay to the west of the Hida Belt, where the Ultra-Tamba and Tamba Belts are distributed. Otoh et al. (1989) reported eastward thrusting (dextral shear) of the belts using asymmetric deformed minor and microstructures in sheared rocks formed in ductile to brittle regimes (Fig. 34). They interpreted the data as indicating that the eastward thrusting resulted from N-NE-directed continental plate movement against N-NW-directed oceanic plate (Izanagi Plate) movement.

Mylonite zone and metamorphic complex of the Hida Belt

Komatsu et al. (1985) regarded the mylonite zone developed along the margin of the Hida

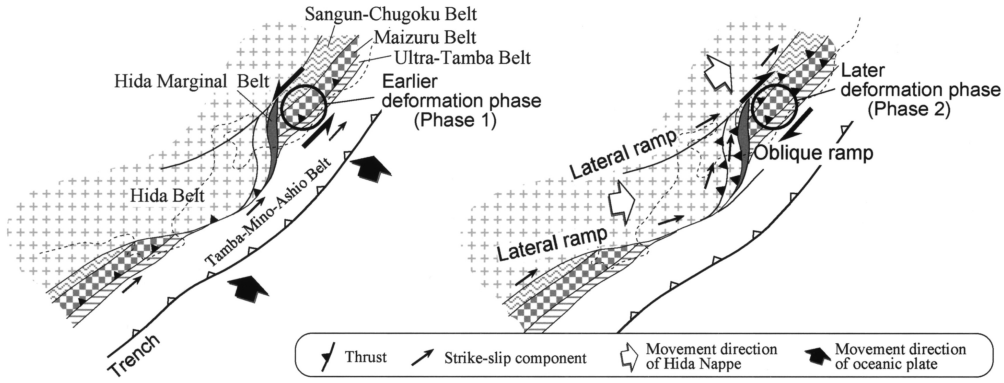

Fig. 35. Map showing the relationship between two deformation phases of the low-grade schist zone and tectonic framework of Japanese Islands in Mesozoic (modified after Takenouchi, 2000). Open-circle area indicates the possible location of the low-grade schist zone in each deformation phase.

Belt as a shear zone formed synchronously with the Hida Nappe emplacement. The mylonite zones are divided into the Unazuki stage (former) mylonites showing S-(C)-C'planar fabrics and the Funatsu stage (later) mylonites showing S-C planar fabrics, which were formed during the Middle to Late Triassic (Komatsu et al., 1993). Komatsu et al. (1993) suggested that the Unazuki stage mylonites were formed as sub-horizontal decollement of NE-directed thrusting of the Hida Belt, and the Funatsu stage mylonites were formed by dextral-reverse movement caused by northward tilting of the Hida Belt (Fig. 34).

Uda et al. (1991) reported the tectonic evolution of the Kuzuryu metamorphic body in the southwestern margin of the Hida Belt, Fukui Prefecture. They concluded that the present arrangement of the metamorphic rocks resulted from a progressive formation process of dextral strike-slip duplex (Fig. 34).

The above structural analyses show thrust movement with dextral shear in the eastern area, with dextral strike-slip movement in the southern and western areas. These local differences in crustal movement can be interpreted by NE-directed nappe feature with a dominant thrust component at an oblique ramp and dominant strike-slip component at a lateral ramp (Fig. 35).

(2) Interaction of continental and oceanic plates

The earlier deformation phase (phase 1 deformation) in the low-grade schist zone consisted of upthrusting with sinistral shear, whereas the later deformation phase (phase 2 deformation) consisted of upthrusting with dextral shear, both of which occurred parallel to the longitudinal direction of the accretionary complex. These inverted shears were considered to indicate a change in the relative movement between the Paleozoic to Mesozoic accretionary

complex (Inner Zone of Southwest Japan) and continental crust (Hida Nappe). If the Hida Nappe thrust over the Inner Zone of Southwest Japan, upthrusting with dextral shear would appear in the accretionary complex. Thus, the later deformation phase is understood to have resulted from reactivation of the Hida Nappe. On the other hand, although oblique subduction of the oceanic plate in the early Cretaceous (Engebretson et al., 1985) may not apply to before the Jurassic, the earlier deformation phase might have resulted from the oblique subduction of the oceanic plate.

Two inverted shear regimes of the low-grade schist zone were caused by alternate movements of the oceanic and continental plates, i.e., oblique subduction of the oceanic plate and oblique upthrusting being reactivation of the Hida Nappe belonging to the continental plate (Fig. 35). The earlier upthrusting with sinistral shear was caused by NE-directed movement of the oceanic plate and the later upthrusting movement with dextral shear was caused by NE-ENE-directed movement of the Hida Nappe. The deformation process of the Paleozoic to Mesozoic accretionary complexes in the Japanese Islands has been considered to have been affected by the oceanic plate only. However, it was influenced by the continental plate in addition to the oceanic plate. The mutual movements of the two plates played an important role in the development of the accretionary complexes of the Japanese Islands.

The process of tectonic disturbance in the Joetsu region may be a unique event reflecting its tectonic situation near the oblique ramp of the Hida Nappe, and is different from those of Southwest Japan to the west of the Fossa Magna region.

Conclusions

1) A once continuous low-grade schist zone was reconstructed by tracing sporadically distributed low-grade schist bodies having common geology, metamorphism, and deformation in the Joestu region showing a complex geological structure.

2) Structural analyses on the basis of geometric and kinematic studies of deformed minor and microstructures developed in the low-grade schist zone divided the whole deformation process into two deformation phases, i.e., the earlier deformation phase (phase 1 deformation) showing a sinistral shear regime with the deformation mechanism of crystal plasticity and diffusive mass transfer, and the later deformation phase (phase 2 deformation) showing a dextral shear regime with the deformation mechanism of fracture, slip, and cataclasis.

3) Deformation facies analysis based on fundamental geometric and kinematic studies showed the temporal and spatial sequences (deformation zoning) of the deformed minorstructures. The former showed that deformed minorstructures formed under conditions of decreasing mean ductility with time, and the latter showed that mean ductility represented by the assemblage of deformed minorstructures decreased with distance from the axial part of a major isoclinal syncline in the western limb. The temporal sequence showing the decrease in mean ductility with time suggested decreases in confining pressure and temperature in

response to rock body exhumation.

4) The two inverted shear regimes were caused by alternate movement of oceanic and continental plates, i.e., oblique subduction of the oceanic plate and oblique upthrusting being reactivation of the Hida Nappe belonging to the continental plate. The former upthrusting with sinistral shear was caused by NE-directed movement of the oceanic plate and the latter upthrusting movement with dextral shear was caused by NE-ENE-directed movement of the Hida Nappe.

5) The deformation processes of the accretionary complexes in the Japanese Islands have been considered to be affected only by oceanic plate. However, the observations presented here indicate that they were influenced by the continental plate in addition to the oceanic plate. The mutual movements of the two plates played an important role in the development of the accretionary complex of the Japanese Islands.

Acknowledgements

I would like to sincere thank to Emeritus Prof. T. Uemura and Dr. T. Toyoshima of Niigata University for continual guidance and discussions throughout this work and for critical reading of the manuscript. I acknowledge Drs. T. Uda and M. Ohkouchi of Niigata University, Drs. F. Takizawa and Y. Takahashi of Geological Survey of Japan for many suggestions and discussions in the field. I would like to thank to Prof. M. Komatsu of Ehime University, Emeritus Prof. K. Chihara of Niigata University and the members of the Niigata Pre-Tertiay Research Group for their valuable discussions. I am grateful to Profs. M. Tateishi, S. Miyashita, Emeritus Profs. Y. Hasegawa and I. Kobayashi of Niigata University for their helpful advices and encouragements. I thank Prof. J. Tazawa for giving the opportunity to contribute the doctoral thesis to the Science Reports.

References

Akamatsu, Y., Kawachi, Y., Muramatsu, T., Shimazu, M. and Tamura, M., 1967, Outline of geology of the environs of the Tanigawa-dake. *Earth Science (Chikyu Kagaku)*, **21**, no. 2, 1-6. (in Japanese)

Arai, F. and Kizaki, Y., 1958, On the Tertiary formations characterized by green tuffs developed in the south of Tanigawa-dake, Jyoetsu district, Pt. 1. Description of the Minakami and Sarugakyo Groups. *Jubli. Publ. Commem. Prof. H. Fujimoto*, 213-219. (in Japanese)

Billings, M. P., 1972, *Structural Geology. 3rd ed.*, Prentice-Hall, New Jergy 606 p.

Caridroit, M., Ichikawa, K. and Charvet, L., 1985, The Ultra-Tamba Zone, a new unit in the Inner Zone of Southwest Japan. - Its importance in the nappe structure after the example of the Maizuru area - . *Earth Science (Chikyu Kagaku)*, **39**, 210-219.

Chihara, K., 1984, Geologic overview of the Joetsu and Ashio Belts (western zone). *Rep. Collab. Res. "Joetsu and Ashio Belts"*, no. 1, 3-23. (in Japanese)

Chihara, K., 1985, Ultramafic rocks in the boundary area between Joetsu and Ashio Belts. *Rep. Collab. Res. "Joetsu and Ashio Belts"*, no. 2, 111-132. (in Japanese)

Chihara, K. and Komatsu, M., 1982, The recent study on the Hida marginal zone, especially the Omi-Renge and the Joetsu belts - a review. *Mem. Geol. Soc. Japan*, no. 21, 101-116. (in Japanese)

Chihara, K. and Komatsu, M., 1992, Geology of the Hakkaisan district. With geological Sheet Map at 1: 50,000, *Geol. Surv. Japan*, 107 p. (in Japanese)

Chihara, K., Komatsu, M., Kurokawa, K. and Imai, N. (1976), Nakanotake hornblende metagabbro in the Sanashigawa Valley, Niigata Prefecture, central Japan (Part 1). *Contri. Dept. Geol. Miner., Niigata Univ*. no. 4, 255-262. (in Japanese)

Chihara, K. and Nishida, S., 1968, Topography and Geology of the Echigo-Sanzan and Okutadami District. *Scientific Report on the Echigo-Sanzan-Okutadami National Park* (Report of Japan Nature Reservation Association, no. 34), 19-55. (in Japanese)

Chihara, K., Shimazu, M., Komatsu, K. and Kurokawa, K., 1977, Geological structure and its development of the western part of the Joetsu Tectonic Belt, central Japan, Part I. Geology. *Sci. Rep., Niigata Univ*., *Ser. E*, no. 4, 1-48. (in Japanese)

Cobbold, P.R. and Quinquis, H., 1980, Development of sheath folds in shear regimes. *Jour. Struct. Geol*., **2**, 119-126.

Dewey, J.F., 1965, Nature and Origin of Kink band. *Tectonophys*., **1**, 459-494.

Engebretson, D. C., Cox, A. and Gordon, R. G., 1985, Relative motions between oceanic and continental plates in the pacific basin. *Geol. Soc. Ame*, *Spec. Pap*., no. 206, 59 p.

Fujimoto, H. and Kobayashi, F., 1961, On the Paleozoic deposits of the Inner Zone of the Ou region. *Jour. Geol. Soc. Japan*, **67**, 221-227. (in Japanese)

Gray, D.R., 1977, Morphological classification of crenulation cleavage. *Jour. Geol*., **85**, 229-235.

Hara, H. and Kashiwagi, K., 2004, Jurassic accretionary complex of the Ashio Terrane in the Kuromatagawa region, Niigata Prefecture, central Japan. *Jour. Geol. Soc. Japan*, **110**, 348-362. (in Japanese)

Hasegawa, Y., 1985, Geologic age of the Pre-Tertiary systems in Omi-Hakuba, Uonuma and Kambara massifs. *Rep. Collab. Res. "Joetsu and Ashio Belts"*, no. 2, 69-84. (in Japanese)

Hayama, Y., Kizaki, Y., Aoki, K., Kobayashi, S., Toya, K. and Yamashita, N., 1969, The Joetsu metamorphic belt and its bearing on the geologic structure of the Japanese Islands. *Mem. Geol. Soc. Japan*, no. 4, 61-82.

Hayasaka, Y., 1987, Study on the late Paleozoic - early Mesozoic tectonic development of western half of the Inner Zone of Southwest Japan. *Geol. Rep., Hiroshima University*, no. 27, 119-204. (in Japanese)

Hayashi, S., Kanzawa, K., Kizaki, Y., Otake, S., Takei, K., Toya, K. and Yamashita, N., 1965, On the Tetori Series found in the upstream of the river Katashinagawa, Gunma Prefecture. *Jour. Geol. Soc. Japan*, **71**, 76-77. (in Japanese)

Henderson, J. R., 1981, Structural analysis of sheath folds with horizontal X-axes, northeast Canada. *Jour. Struct. Geol*., **3**, 203-210.

Ishiga, H., 1986, Ultra-Tamba Zone of Southwest Japan. *Jour. Geosci., Osaka City Univ*., no. 29. 45-88.

Johnson, A. M., 1977, *Styles of folding*. Elsevier, Amsterdam, etc. 406 p.

Kimura, T., 1952, On the Geological Study of the Iwamuro Formation, Tone Gun, Gunma Prefecture, Series 1. *Jour. Geol. Soc. Japan,* **58**, 457-468. (in Japanese)

Kimura, G. and Mukai, A., 1991, Underplated units in an accretionary complex : Melange of the Shimanto belt of eastern Shikoku, southwest Japan, *Tectonics*, **10**, 31-50.

Kobayashi, F., 1955, Geology of the riverhead district of the Tone River. *Jour. Geogr*., **64**, 96-102. (in Japanese)

Komatsu, M., 1990, Hida-Gaien Belt and Joetsu Belt. *In* Ichikawa, K., Mizutani, S., Hara, I., Hada, S. and Yao, A. eds., *Pre-Cretaceous Terranes of Japan*. Publicaion of IGCP 224,

Nippon Insatsu Shuppan, Osaka, 25-40.
Komatsu, M., Nagase, M., Naito, K., Kanno, T., Ujihara, M. and Toyoshima, T., 1993, Structure and Tectonics of the Hida massif, central Japan. *Mem. Geol. Soc. Japan*, no. 42, 39-62. (in Japanese)
Komatsu, M., Ujihara, M. and Chihara, K., 1985, Pre-Tertiary basement structure in the Inner zone of Honshu and the North Fossa Magna region. *Contri. Dept. Geol. Miner., Niigata Univ*. no. 5, 133-148. (in Japanese)
Komatsu, M., Ujihara, M., Takenouchi, K., Uda, T. and Uemura, T., 1988, Funatsu shear zone - dextral strike slip zone along the margin of the Hida complex. *Prof. Shinji Sato Mem. Vol. Ehime Univ*., 27-37. (in Japanese)
Mackenzie, J. S., Needham, D. T. and Agar, S. M., 1987, Progressive deformation in accretionary complex : an example from the Shimanto belt of eastern Kyushu, southwest Japan. *Geology*, **15**, 353-356.
Maeda, S., 1962, On the crystalline schists on the boundary of Gunma and Niigata Prefectures. *Jour. Geol. Soc. Japan*, **68**, 407. (in Japanese)
Matsumoto, Y., Sashida, K. and Hori, N., 2001, Paleozoic and Mesozoic radiolarians from the area east of Koide Town, Kitauonuma Country, Niigata Prefecture, central Japan. *News of Osaka Micropaleontologists (NOM), Spec. vol.,* no. 12, 99-112. (in Japanese)
Minnigh, L. D., 1979, Structural analysis of sheath-folds in a meta-chert from the Western Italian Alps. *Jour. Struct. Geol*, **1**, 275-282.
Mizutani, S., Uemura, T. and Yamamoto, H., 1984, Jurassic radiolarians from the Tsugawa area, Niigata Prefecture, Japan. *Earth Science (Chikyu Kagaku)*, **38**, 352-358.
Niigata Pre-Tertiary Research Group, 1986, Ashio Belt in the rivers Sodezawa and Shiratogawa areas, Okutadami. *Rep. Collab. Res. "Joetsu and Ashio Belts"*, no. 3, 69-75. (in Japanese)
Niigata Pre-Tertiary Research Group, 1996, Geology of River Sodezawagawa area, Okutadami, Japan. *Rep. Collab. Res. "Significance of greenstone on accretion tectonics"*, no. 1, 127-133. (in Japanese)
Nishimura, Y., 1998, Geotectonic subdivision and areal extent of the Sangun belt, Inner Zone of Southwest Japan. *Jour. Metamorphic Geol*., **16**, 129-140.
Ohkouchi, M., Takenouchi, Okuda, E. and K., Uda, T., 2002, Significance of pelitic schist from the Nakanotake metagabbroic mass, Katashina Belt, central Japan. *Earth science (Chikyu Kagaku)*, **56**, 295-300.
Otoh, S., Tsukada, K., Kasahara, K., Hotta,, K. and Sasaki, M., 2003, Outline of the shear zones in the Hida Marginal Belt. *Mem. Fukui Prefectural Dinosaur Mus.*, no. 2, 63-73.
Otoh, S., Yanai, S. and Yamakita, S., 1989, Mesozoic ductile thrusting in the Tamba and Ultra-Tamba Zones; its implication in the plate kinematics of the Far East. *Structural Geology (The Journal of the Tectonic Research Group in Japan)* , no. 34, 75-84. (in Japanese)
Otsuka, T., 1989, Mesoscopic folds of chert in Triassic -Jurassic chert-clastic sequence in the Mino Terrane, central Japan. *Jour. Geol. Soc. Japan*, **95**, 97-111.
Passchier, C. W. and Trouw, R. A. J. (1996), *Microtectonics*. Springer, Berlin, Heidelberg, New York, 289 p.
Paterson, S. R. and Sample, J.C., 1988, The development of folds and cleavges in slate belts by underplating in accretionary complex : a comparison of the Kodiak formation, Alaska and the Caraveras complex, California. *Tectonics*, **7**, 859-874.
Ramsay, J. G., 1967, *Folding and Fracturing of rocks*. McGraw-Hill, N. Y., Lond. 568 p.
Research Group of the Asahi Mountains, 1987, Geology of southwestern part of the Asahi Mountains, North-east Japan - Part I. Petrography and mutual relations of rocks -. *Earth Science (Chikyu Kagaku)*, **41**, 253-280. (in Japanese)
Sample, J. C. and Moore, J. C., 1987, Structural style and kinematics of an underplated slate

belt, Kodiak and adjacent islands, Alaska. *Bull. Geol. Soc. Amer.*, **99**, 7-20.
Sander, B., 1930, *Gefuegekunde der Gesteine*. Springer, Vienna, 352 p.
Sato, N. and Komatsu, M., 1985, Tokura Ophiolite of the Katashina Belt. *Rep. Collab. Res,"Joetsu and Ashio Belts"*, no. 2, 133-139. (in Japanese)
Sato, T., Yoshida, S. and Kimura, T., 1975, Permian-Triassic in the Kuromatagawa area, Niigata Prefecture. *Jour. Geol. Soc. Japan*, **81**, 709-711. (in Japanese)
Shimizu, Y., Ishiwatari, A. and Tsujimori, T., 2000, Glaucophane schists pebbles from the Miocene Awazawa Formation in Minakami Town, the Joetsu metamorphic belt, central Japan. *Abstr. 107th Ann. Meet. Geol. Soc. Japan*, 289. (in Japanese)
Shimizu, Y., Ishiwatari, A. and Tsujimori, T., 2001, Pelitic schists pebbles from the Miocene Awazawa Formation in Minakami area, the Joetsu metamorphic belt, central Japan. *Abstr. 108th Ann. Meet. Geol. Soc. Japan*,160. (in Japanese)
Soma, T. and Yoshida, M., 1964, The Tanigawadake plutonic complex. *Jour. Mineral. Petrol. Econ. Geol.*, **51**, 39-52. (in Japanese)
Taira, A., Katto, J., Tashiro, M., Okamura, M. and Kodama, K., 1988, The Shimanto belt in Shikoku, Japan - Evolution of Cretaceous to Miocene accretionary prism. *Modern Geol.*, **12**, 5-46.
Takagi, H. and Kobayashi, K., 1996, Composite planar fabrics of fault gouges and mylonite-comparative petrofabrics. *Jour. Geol. Soc. Japan*, **102**, 170-179. (in Japanese)
Takagi, H. and Hara, T., 1994, Kinematic pictures of the ductile shear zones in the Hida terrane and their tectonic implication. *Jour. Geol. Soc. Japan*, **100**, 931-950. (in Japanese)
Takahashi, Y., 1998, Geology and structure of the Nihonkoku Mylonite Zone on the borders of Niigata and Yamagata Prefectures, northeast Japan. *Jour. Geol. Soc. Japan*, **104**, 122-136. (in Japanese)
Takahashi, Y., Toyoshima, T., Shimura, T., Hara, H., Takeuchi, K., Sakai, A. and Nakano. S., 2004, *Geology of the Suhara district*. Quadrangle Series, 1:50,000, Geological Survey of Japan, AIST, 80 p. (in Japanese)
Takami, M., Nishimura, Y. and Isozaki, Y., 1992, Weakly metamorphosed Jurassic accretionary complex with 170 Ma K-Ar age in eastern Yamaguchi Prefecture, southwest Japan. *Abstr. 99th Ann. Meet. Geol. Soc. Japan*, 129. (in Japanese)
Takenouchi, K., 1985, Deformation facies and series of the Mizunashigawa metamorphic rocks, Niigata Prefecture. *Structural Geology (The Journal of the Tectonic Research Group in Japan)* , no. 31, 9-16. (in Japanese)
Takenouchi, K., 1988, The constitution and deformation facies of the Mizunashigawa metamorphic rocks, central Japan. *Jour. Geol. Soc. Japan*, **94**, 479-491. (in Japanese)
Takenouchi, K., 2000, Two deformation phases and two uplifting stages of the Jurassic Mizunashigawa metamorphic rocks, Ashio Belt, central Japan. *Jour. Geol. Soc. Japan*, **106**, 743-761. (in Japanese)
Takenouchi, K., 2004, Deformation sequences of the Omi schists (Hida Gaien Belt) on the basis of deformation facies analysis, central Japan. *Jour. Geol. Soc. Japan*, **110**, 608-619. (in Japanese)
Takenouchi, K. and Takahashi, Y., 2002, Deformation history of low-grade schists in the Joetsu region, central Japan -Correlation between the Kawaba and Mizunashigawa metamorphic rocks. *Jour. Geol. Soc. Japan*, **108**, 794-805.
Takizawa, F and Sato, K., 1986, Reexamination of 'Mesozoic strata' around Mt. Tanigawadake. *Rep. Collab. Res. "Joetsu and Ashio Belts"*, no. 3, 76-83. (in Japanese)
Tazawa, J. and Niigata Pre-Tertiary Research Group, 1999, Permian Brachiopoda from the Okutadami area near the boundary between Niigata and Fukushima Prefectures, central Japan and their tectonic implications. *Jour. Geol. Soc. Japan*, **105**, 729-732. (in Japanese)

Uda, T., Hosaka, H. and Kobayashi, K., 1991, Strike-slip duplex of Kuzuryu metamorphic complex, central Japan. *Sci. Rep., Niigata Univ*., *Ser. E*, no. 8, 109-123.

Uemura, T., 1981, Deformation facies, series and grades. *Jour. Geol. Soc. Japan*, **87**, 297-305.

Uemura, T., 1984, Deformation facies of some shear belts in Japan. *29th IGC Abstracts Vol. 3*, *Sect. 7*, 442-443.

Uemura, T., 1992, On the facies of deformation structure. *Jour. Geol. Soc. Japan*, **98**, 1073-1084. (in Japanese)

Uemura, T., Hasegawa, Y. and Misaki, T., 1984, Conodont fossils from the river Kuromatagawa area. *Rep. Collab. Res. "Joetsu and Ashio Belts*", no. 1, 41-43. (in Japanese)

Uemura, T. and Long. X., 1987, Kink bands in rocks. *Jour. Geol. Soc. Japan*, **93**, 681-699. (in Japanese)

Uemura, T. and Takashima, T., 1985, Basement rocks of the Mt. Kamigongendoyama area in the Uonuma Massif. *Rep. Collab. Res. "Joetsu and Ashio Belts"*, no. 2, 41-45. (in Japanese)

Uemura, T. and Takenouchi, K., 1984, Deformation facies analysis of the Mizunashigawa metamorphic rocks. *Rep. Collab. Res. "Joetsu and Ashio Belts",* no. 1, 24-29. (in Japanese)

Uemura, T. and Takenouchi, K., 1986, Note on deformation facies -Mizunashi-gawa metamorphic rocks, central Japan. *Sci. Rep., Niigata Univ.*, *Ser. E*, no. 7, 89-101.

Uemura, T., Uda, T. and Long. X., 1985, Note on deformation facies -Ohmi crystalline schist, central Japan. *Sci. Rep., Niigata Univ., Ser. E*, no. 6, 1-15.

Uemura, T. and Yokota, Y., 1981, Deformation facies of the folded Jurassic Kuruma Group, central Japan. *Earth Science (Chikyu Kagaku)*, **35**, 41-48.

Yamada, H. and Kurokawa, K., 1985, Finding of Jurassic radiolarians from chert at Oshirakawa, Irihirose, Niigata Prefecture. *Rep. Collab. Res. "Joetsu and Ashio Belts"*, no. 2, 5-9. (in Japanese)

Yamamoto, T., Takizawa, F., Takahashi, Y., Kubo, K., Komazawa, M., Hiroshima, T. and Sudo, S., 2000, *Geological Map of Japan 1:200,000, Nikko.* Geological Survey of Japan. (in Japanese)

Yamashita, N. ed., 1995, *Fossa Magna.* Tokai Univ. Press, Tokyo. 310 p. (in Japanese)

Yanagisawa, Y., Kobayashi, I., Takeuchi, K., Tateishi, M., Chihara, K. and Kato, H., 1986, *Geology of the Ojiya district.With Geological Sheet Map at 1:50,000,* Geol. Surv. Japan, 177 p. (in Japanese)

Yano, K., Ishida, K., Namiki, H., Sakamoto, K. and Kato, T., 1993, New findings of a formation corresponding to the Ultra Tamba Zone to the east of the Fossa Magna. *Abstr. 100th Ann. Meet. Geol. Soc. Japan*, 456. (in Japanese)

Yokoyama, K., 1992, K-Ar ages of metamorphic rocks at the top of Mt. Tanigawa-dake, central Japan. *Bull. Natn. Sci. Mus*., *Ser. C*, **17**, 43-47.

Yoshimura, T. and Ichihashi, K., 1966, Pebbles of metamorphic rocks in the Awasawa Formation (Neogene Tertiary) distributed in Minakami-machi, Gunma Prefecture. *Contr. Dept. Geol. Miner., Niigata Univ*., no. 1, 97-104. (in Japanese)